The Abdus Salam
International Centre for Theoretical Physics

United Nations
Educational, Scientific
and Cultural Organization

International Atomic
Energy Agency

SMR.1771 -7

Conference and Euromech Colloquium #480

on

High Rayleigh Number Convection

4 - 8 Sept., 2006, ICTP, Trieste, Italy

Cascades, Decoherence & Plumes in turbulent thermal convection

Ke Qing Xia
The Chinese University of Hong Kong
Hong Kong

Cascades, Decoherence and Plumes in Turbulent Thermal Convection

Ke-Qing Xia

Department of Physics

The Chinese University of Hong Kong

Conference & Euromech Colloquium #480 on High Rayleigh Number Convection

Trieste, Italy, 4-8 September 2006

Acknowledgement

Chao Sun

Heng-Dong Xi

Quan Zhou

Work supported by
the Research Grants Council of Hong Kong
(Project No. CUHK403003, 403705).

Several issues in turbulent convection

- **Heat transport**
- **Statistics of turbulent fluctuations**
- **Flow structure and dynamics**
- **Coherent structures**

Specific issues addressed in this talk:

- **Cascades of velocity and temperature fluctuations**

Measurements of real-space velocity and temperature structure functions

- **De-coherence of LSC:**

Cessations and Flow mode transitions

- **Plumes:**

Extraction and characterization of plumes as individual geometrical and thermal objects.

Part 1

Cascades of velocity and temperature fluctuations

A long-standing issue:

What is the mechanism that drives the velocity and temperature cascades in turbulent thermal convection, or, in general, buoyancy-driven thermal turbulence?

Different dynamics may be manifested as different scaling laws for the velocity and temperature structure functions

What are the true scaling exponents of the structure functions?

Bolgiano-Obukhov Scaling (1959)

$$\eta << \ell << L$$

$$v_\ell = v(x+\ell) - v(x)$$

$$S_p(\ell) \equiv \left\langle v_\ell^p \right\rangle$$

$$T_\ell = T(x+\ell) - T(x)$$

$$R_p(\ell) \equiv \left\langle T_\ell^p \right\rangle$$

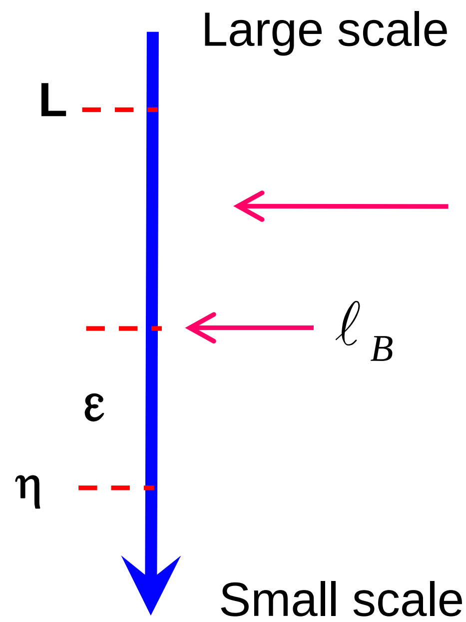

Buoyancy Effect is more important than energy dissipation

K41 $\begin{cases} \ell < \ell_B \\ S_p(\ell) \sim \ell^{p/3} \\ R_p(\ell) \sim \ell^{p/3} \end{cases}$

BO59 $\begin{cases} \ell > \ell_B \\ S_p(\ell) \sim \ell^{\frac{3p}{5}} \\ R_p(\ell) \sim \ell^{\frac{p}{5}} \end{cases}$

Scaling behavior in convective thermal turbulence: previous works

Many studies have been made on this subject.

Procaccia & Zeitak, RPL(1989); L'vov, PRL (1991)
Wu, Kadanoff, Libchaber & Sano, PRL(1990);
Castaing, PRL (1990)
Shraiman & Siggia, PRA(1990);
Grossmann & Lohse, PRL(1991);
Tong & Shen PRL(1992);
Brandenburg PRL (1992); Yakhot, PRL (1992) ;
Cioni, Ciliberto & Sommeria, Europhys. Lett. (1995).
Kerr, JFM(1996)
Benzi, Toschi & Tripiccione, J. Stat. Phys. (1998)
Ashkenazi & Steinberg, PRL(1999);
Glazier et al. Nature (1999), Mashiko,Tsuji, Mizuno & Sano, PRE(2004);
Skrbek, Niemela, Sreenivasan & Donnelly,Nature (2000), PRE(2002);
Calzavarini, Toschi & Tripiccione, PRE (2002).
Ching, PRE (2000); Ching et al. JoT(2004)
Zhou & Xia, PRL(2001) Shang & Xia, PRE(2001);
Calzavarini, Toschi & Tripiccione, PRE(2002);
Camussi & Verzicco, Euro. J. Mech. (2004);

Several theoretical models give BO scaling and many experimental and numerical results found apparent BO scaling exponent

But there are also many theoretical arguments and numerical evidences against it

In the studies that appear to have observed BO59, some are based on very limited scaling range or data precision, while many others based on data obtained in the time/frequency domain. All theoretical predictions are in space domain.

Time domain $\longrightarrow$ Space domain

Taylor hypothesis

$$\frac{u'}{U} << 1$$

$$\ell = U\tau$$

$$\frac{u'}{U} \sim 1\,(sidewall)$$

$$\frac{u'}{U} >> 1\,(center)$$

To determine the true scaling properties of the temperature and velocity fields direct real-space measurements of the structure functions are needed.

Experimental Setup:

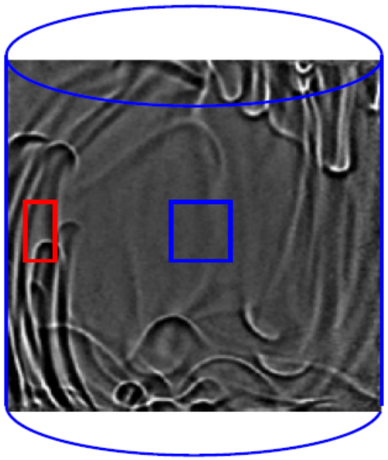

Center:
few plumes

Sidewall:
plume dominant region

Two regions may have different scaling behavior!

Velocity measurement

Ra=7x10^9, Pr = 4.3

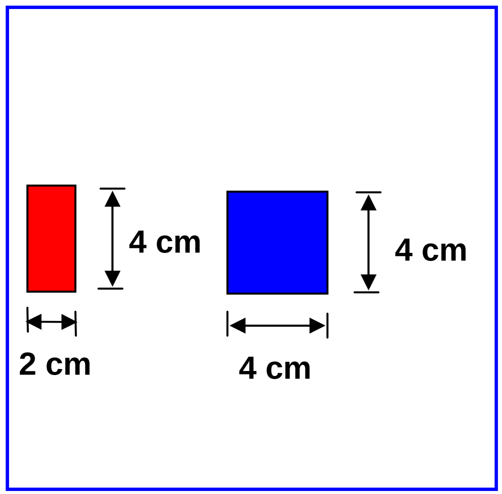

PIV vector maps: 7500
(1 hour with data rate 2.2 Hz)

Spatial resolution:
0.66 mm

Temperature measurement

Ra = 1x10^{10}, Pr = 4.3

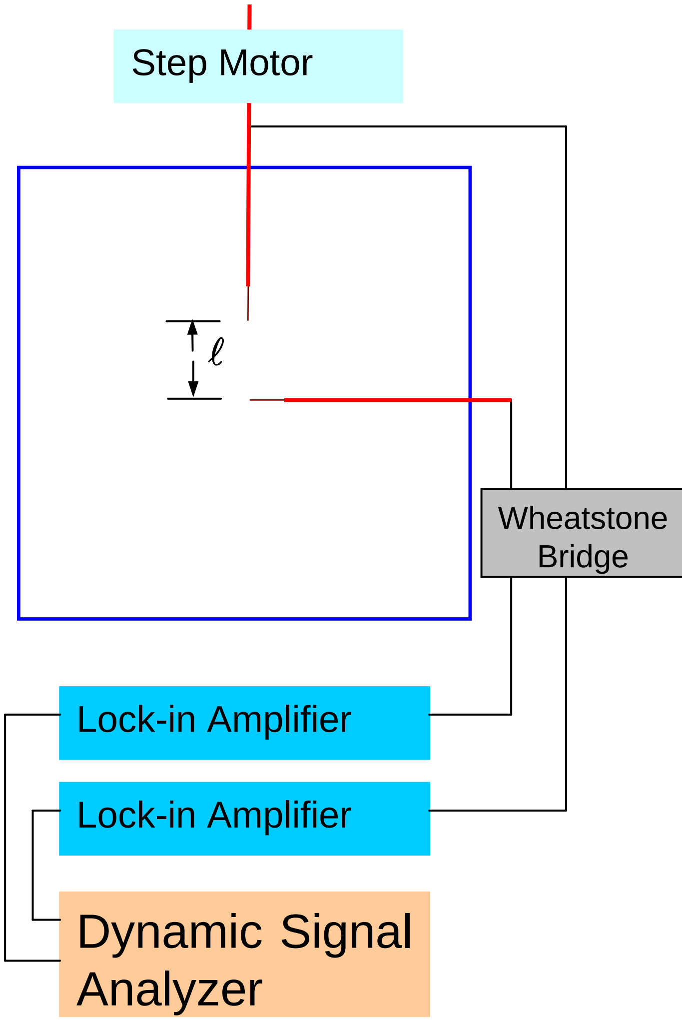

***l*: from 0.5 mm to 90 mm**
***Each l*: Data rate=32Hz, Data length:**1,152,000

PIV can acquire a large amount of data for statistical calculation over a reasonable time frame

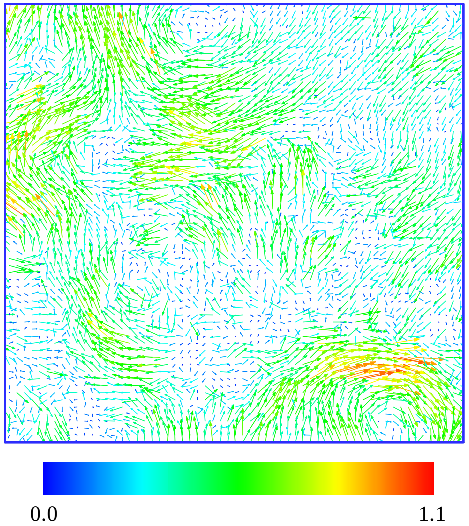

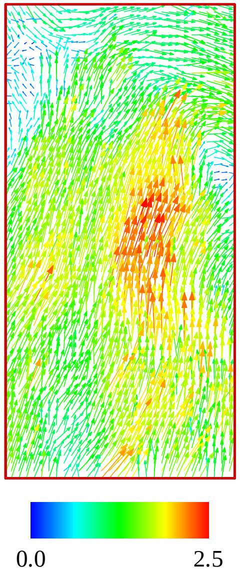

Center: 61x61x7500 data points

# of velocity differences:

24,700,000 for smallest r in inertial region.

12,600,000 for largest r in inertial region

Sidewall:61x30x7500 data points

# of velocity differences:

15,100,000 for smallest r in inertial range.

3,720,000 for largest r in inertial region

Definition of structure functions (SF)

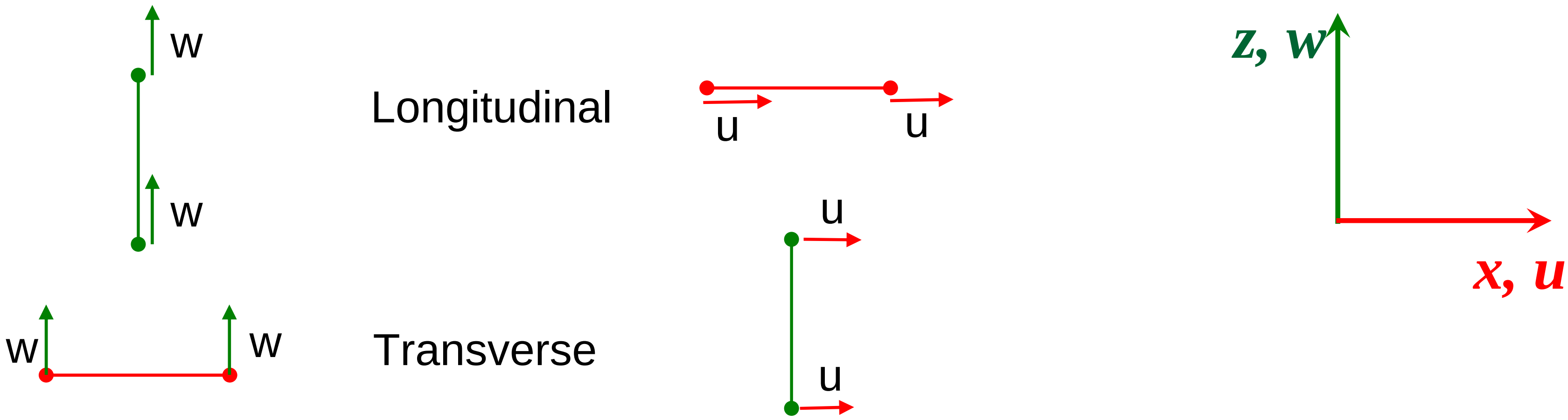

Longitudinal SF of vertical velocity

$$S_p^{L,w}(r) = \left\langle \left| w(x, z+r) - w(x, z) \right|^p \right\rangle$$

Transverse SF of vertical velocity

$$S_p^{T,w}(r) = \left\langle \left| w(x+r, z) - w(x, z) \right|^p \right\rangle$$

Longitudinal SF of horizontal velocity

$$S_p^{L,u}(r) = \left\langle \left| u(x+r, z) - u(x, z) \right|^p \right\rangle$$

Transverse SF of horizontal velocity

$$S_p^{T,u}(r) = \left\langle \left| u(x, z+r) - u(x, z) \right|^p \right\rangle$$

Data convergence and SFs in cell center

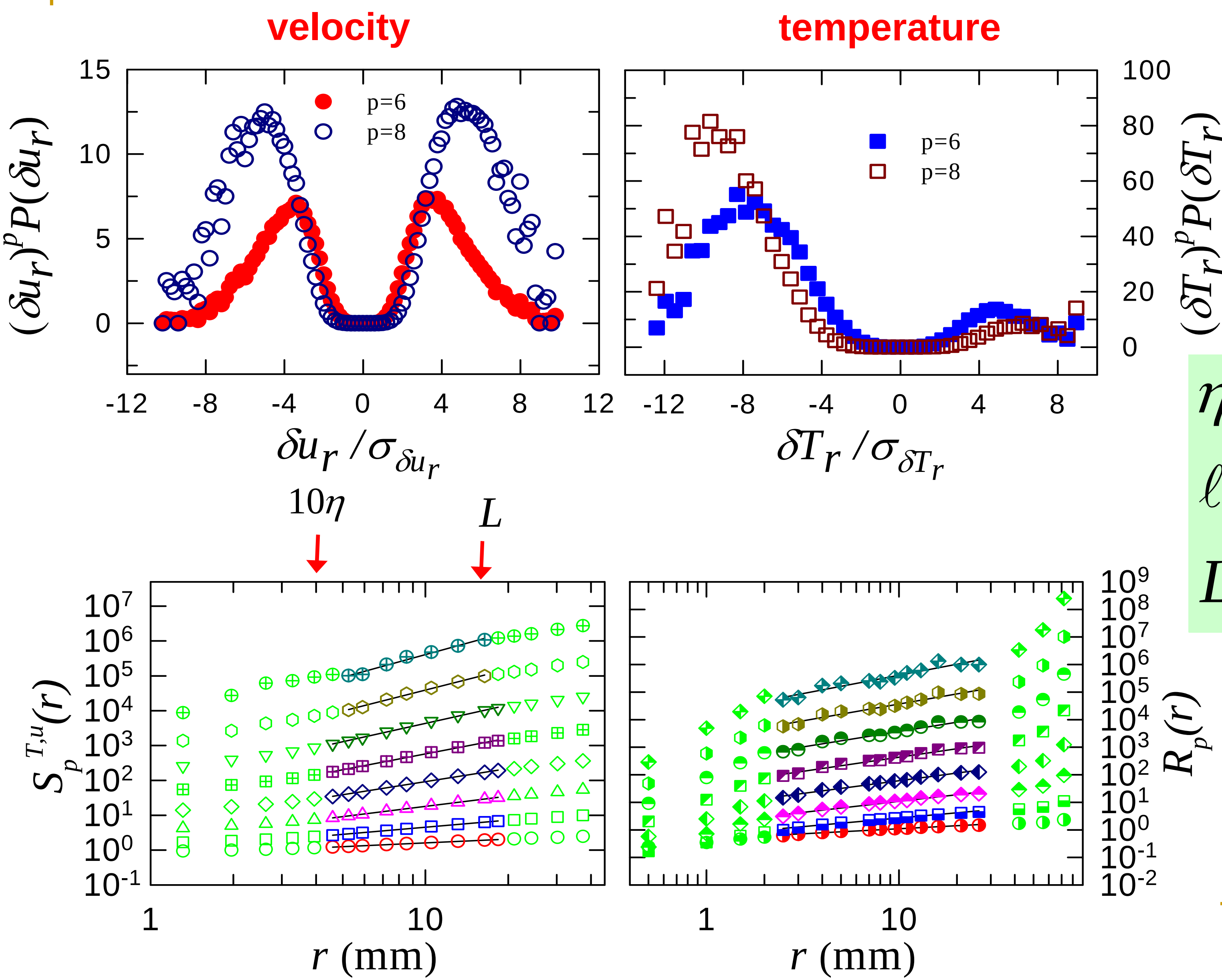

$$\eta \approx 0.4\ mm$$

$$\ell_B \approx 5\ mm$$

$$L = 14.4\ mm$$

SFs in center

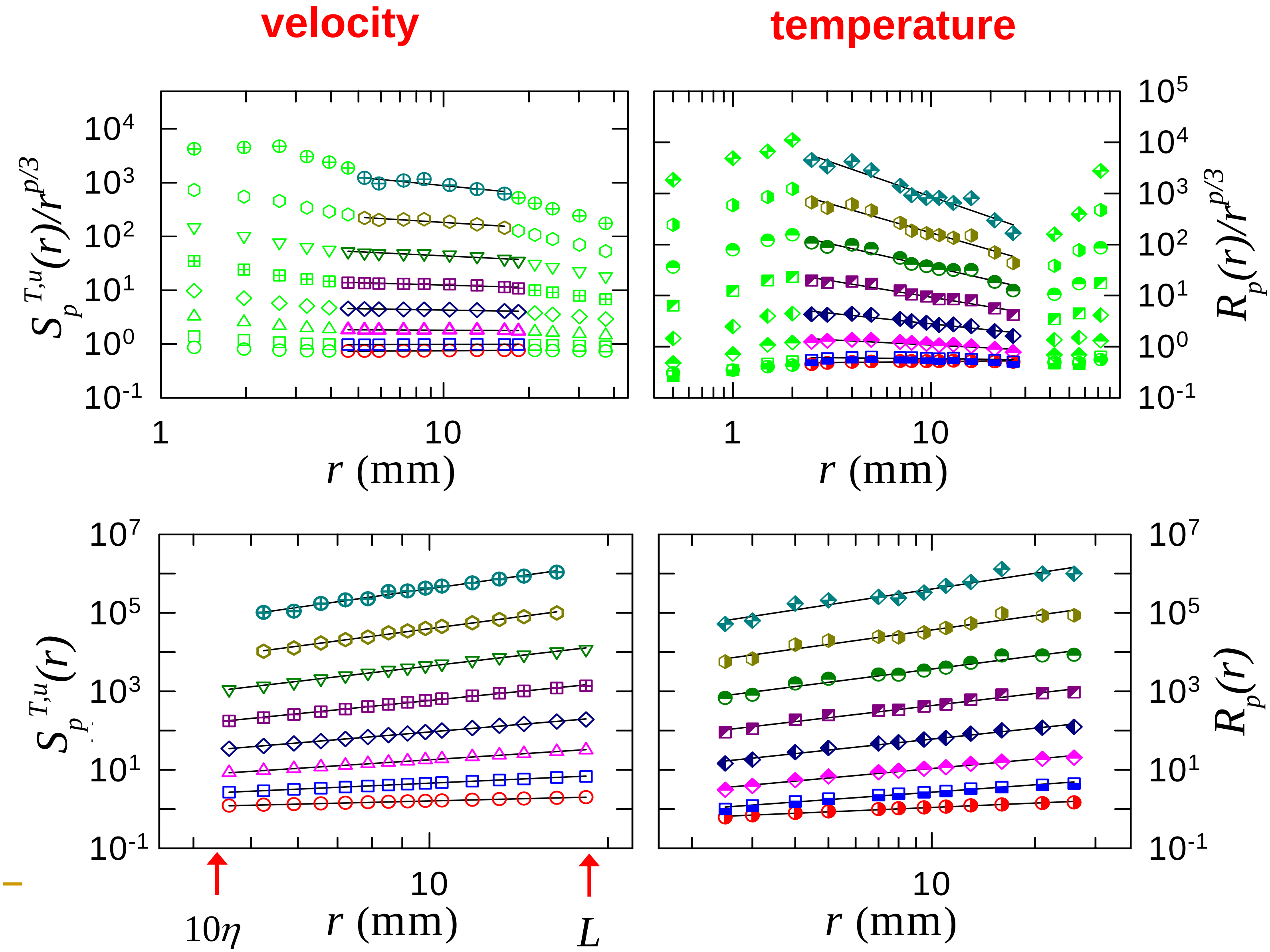

SFs near sidewall

Inertial range is longer than in center

velocity **temperature**

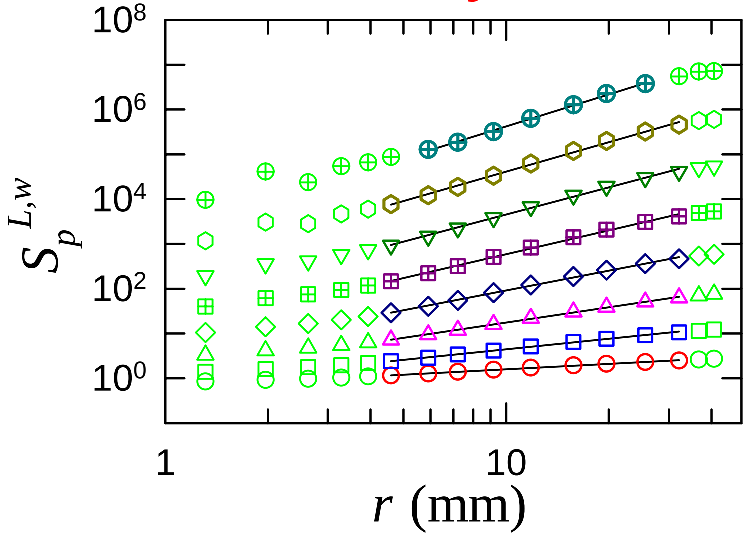

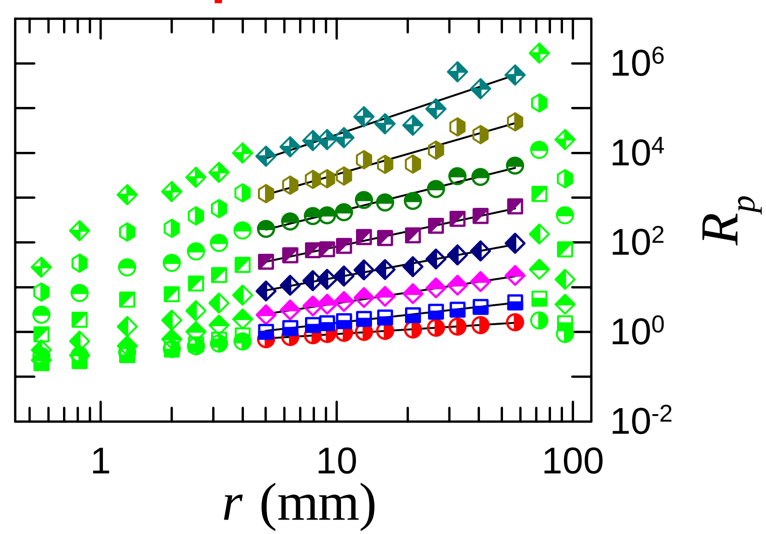

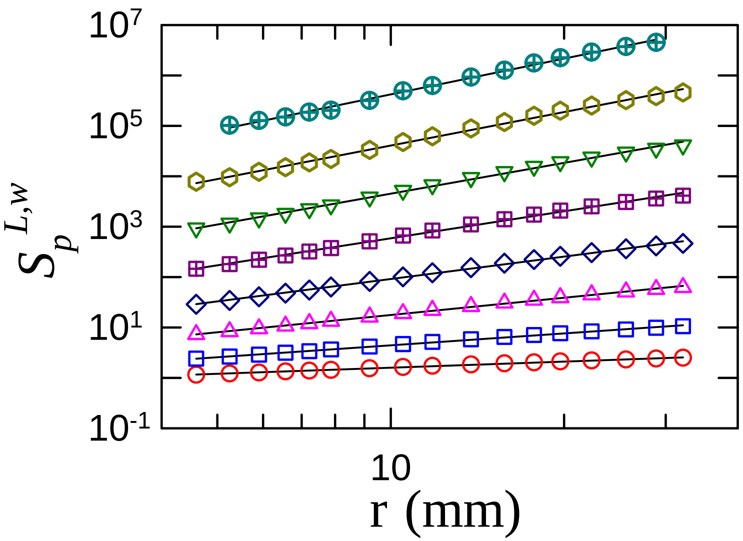

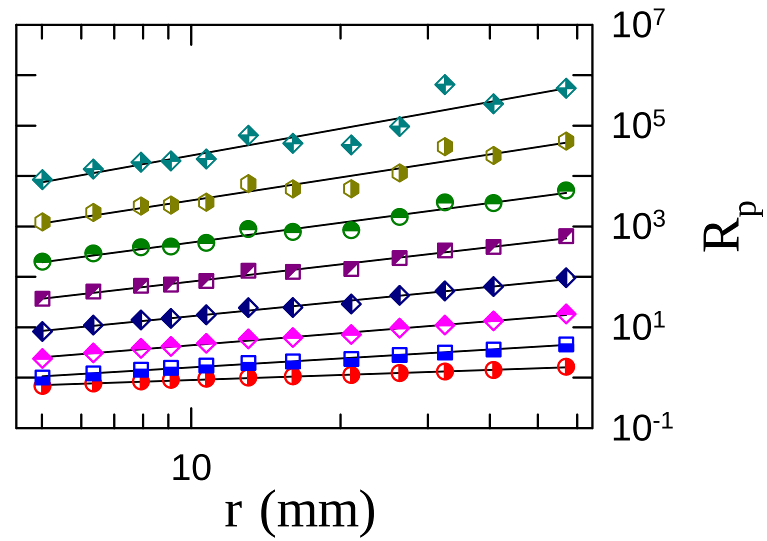

SF exponents

	Center					Sidewall		
p	$\zeta_p^{L,w}$	$\zeta_p^{T,w}$	$\zeta_p^{T,u}$	$\zeta_p^{L,u}$	ξ_p	$\zeta_p^{L,w}$	$\zeta_p^{T,u}$	ξ^p
1	0.35±0.01	0.35±0.01	0.36±0.01	0.36±0.01	0.37±0.01	0.40±0.01	0.38±0.01	0.33±0.01
2	0.68±0.01	0.68±0.01	0.68±0.01	0.68±0.01	0.63±0.01	0.78±0.01	0.72±0.01	0.59±0.01
3	0.99±0.01	1.00±0.01	0.98±0.01	0.98±0.01	0.80±0.01	1.14±0.01	1.01±0.01	0.80±0.01
4	1.25±0.02	1.27±0.02	1.26±0.02	1.25±0.02	0.93±0.01	1.48±0.02	1.27±0.02	0.97±0.01
5	1.53±0.03	1.51±0.03	1.52±0.03	1.53±0.03	1.03±0.01	1.78±0.03	1.52±0.04	1.13±0.02
6	1.81±0.04	1.73±0.04	1.76±0.04	1.76±0.04	1.12±0.02	2.03±0.04	1.70±0.06	1.31±0.02
7	2.02±0.06	1.96±0.06	2.00±0.06	1.99±0.06	1.22±0.04	2.21±0.06	1.94±0.08	1.52±0.04
8	2.30±0.10	2.09±0.10	2.14±0.10	2.07±0.10	1.33±0.05	2.36±0.08	2.05±0.13	1.77±0.05

Velocity fluctuations in central region appear to be isotropic.

Statistical characteristics in cell center

Condition for local isotropy:

$$S_2^T = S_2^L + \frac{1}{2} r \frac{\partial}{\partial r} S_2^L$$

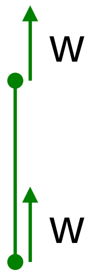

Longitudinal

Transverse

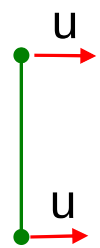

$$S_2^T = (1 + 0.68/2) S_2^L = 1.34 S_2^L$$

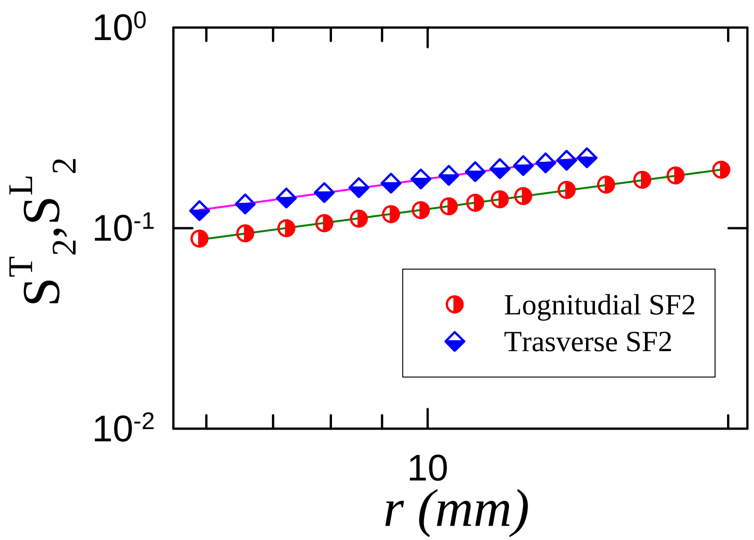

$$w: \; S_2^T / S_2^L = 1.31 \pm 001$$

$$u: \; S_2^T / S_2^L = 1.34 \pm 0.02$$

Cell center: nearly isotropic.

Scaling behavior in cell center

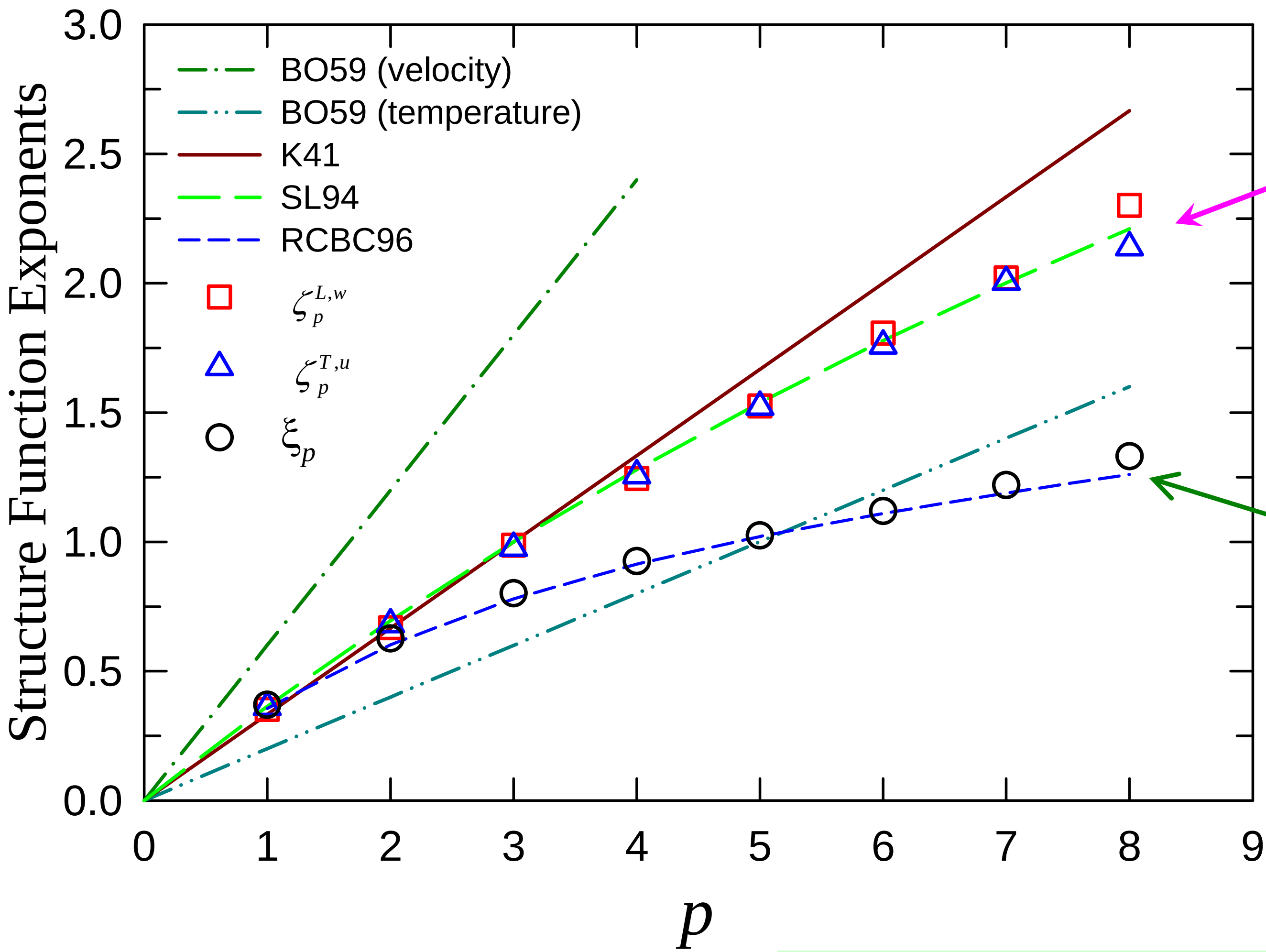

Velocity: homogeneous and isotropic Navier-Stokes turbulence with intermittency corrections.

Temperature: a **passive** scalar in homogeneous and isotropic NS turbulence.

SL94 —— **She & Leveque PRL (1994)** $\zeta_p = p/9 + 2[1 - (\frac{2}{3})^{p/3}]$

RCBC96 —— **Ruiz-Chavarria, Baudet & Ciliberto, Physica D (1996)** $\xi_p = 0.06p + 0.8(1 - 0.63^p)$

Scaling behavior near sidewall: vertical direction

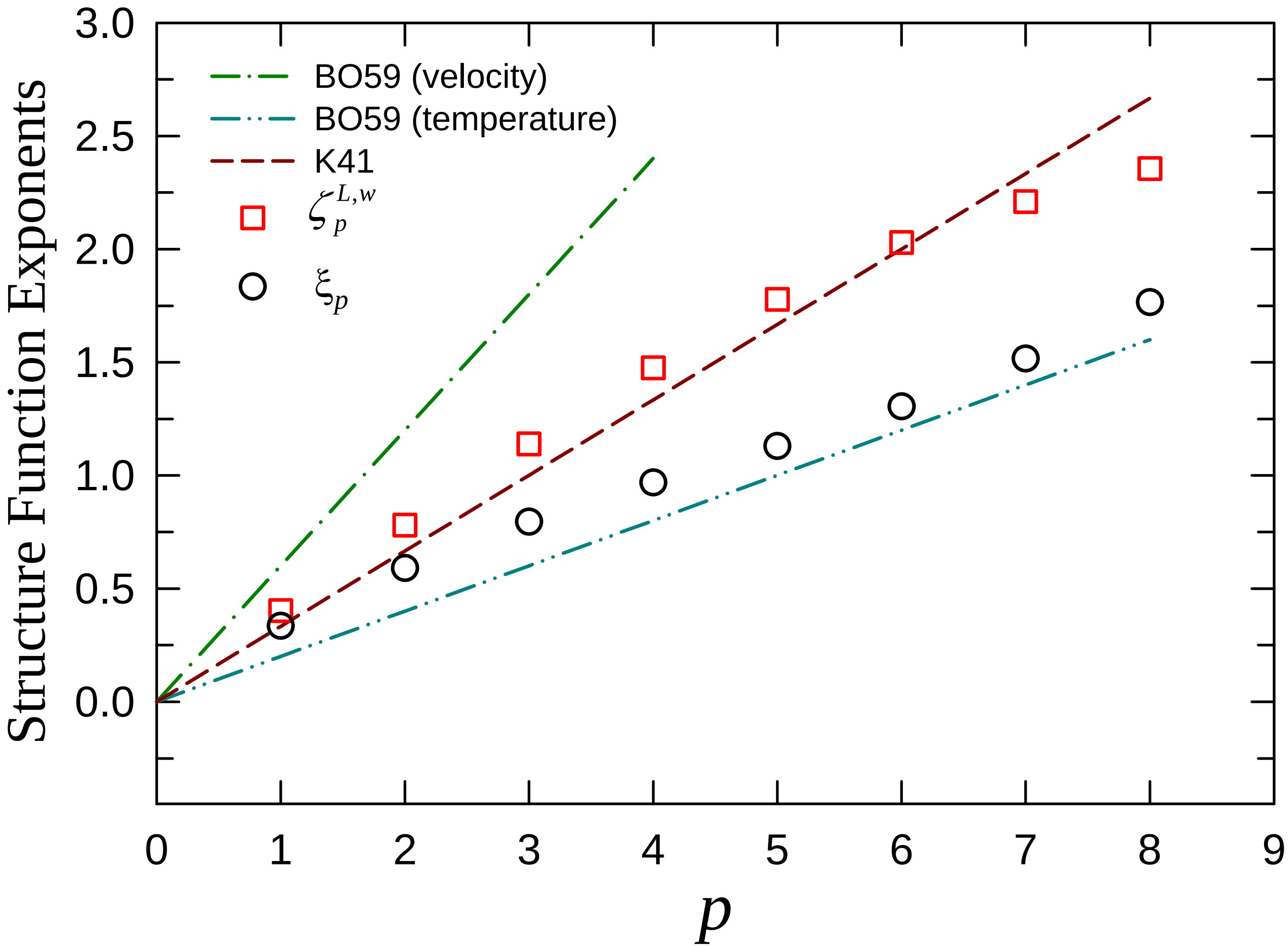

Neither BO59 nor K41

Dimension model

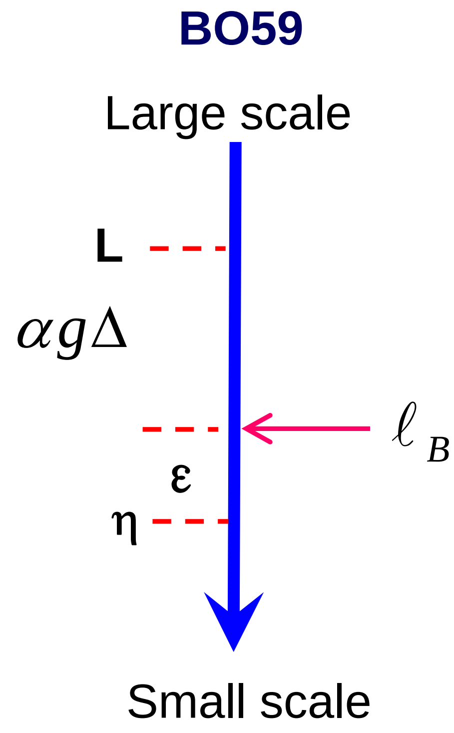

$$\frac{\partial \vec{u}}{\partial t} + \vec{u} \cdot \nabla \vec{u} = -\frac{1}{\rho} \nabla p + \nu \nabla^2 \vec{u} - g \alpha \Delta T \hat{z}$$

Both dissipation and buoyancy influence the cascade.

Assume ε_v and $\alpha g \Delta$ are equally important:

$$v_\ell^p \sim \ell^\alpha (\alpha g \Delta \varepsilon_v)^\beta = \ell^{\frac{2p}{5}} (\alpha g \Delta \varepsilon_v)^{\frac{p}{5}} \sim \ell^{\frac{2p}{5}}$$

$$T_\ell^p \sim \ell^a (\alpha g \Delta \varepsilon_v)^b \varepsilon_\theta^c = \ell^{\frac{3p}{10}} (\alpha g \Delta \varepsilon_v)^{-\frac{p}{10}} \varepsilon_\theta^{\frac{p}{2}} \sim \ell^{\frac{3p}{10}}$$

Scaling behavior near sidewall: vertical direction

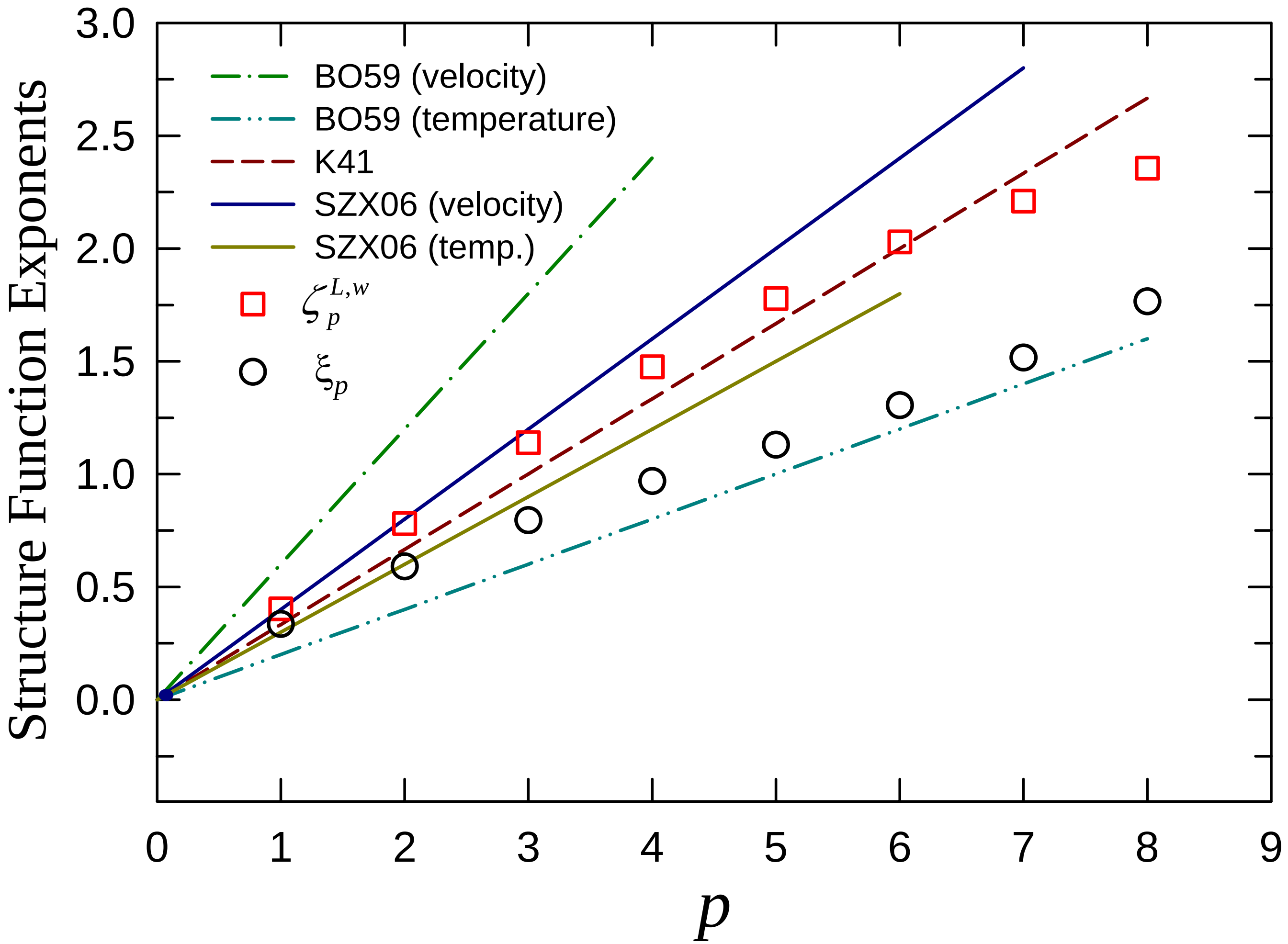

High order structure functions are influenced by intermittency effect, low order SFs can better test the dimensional model.

Fractional SFs

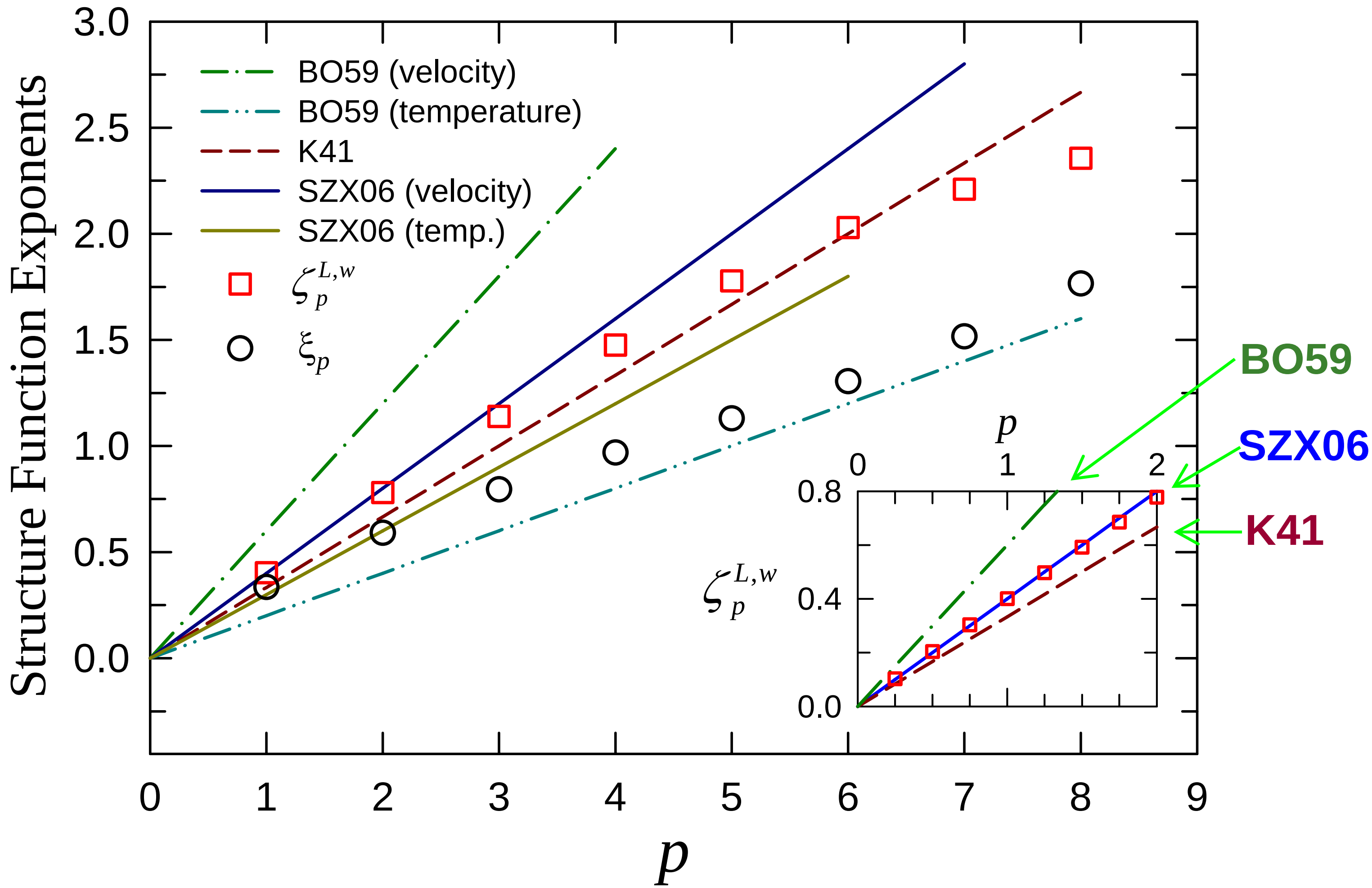

Excellent agreement between our model with experimental results for fractional SFs,

Summary for Part 1

Cell center: Turbulent flow is locally isotropic

Velocity behaves the same as in homogeneous and isotropic NS turbulence. SF exponents may be described by the hierarchy model for velocities (SL94).

Temperature behaves as a passive scalar in NS turbulence. SF exponents may be described by the hierarchy model for passive Scalars (RCBC96).

Sidewall: Turbulent flow is locally anisotropic.

Vertical velocity and temperature follow neither BO59 nor K41. SF exponents may be described by a dimension model treating buoyancy and viscous dissipation on an equal footing.

High order SF deviate from dimensional model due to intermittency.

Test of crossover effect. Constraints on future models

PRL (accepted)

Part 2

Cessations and Decoherence of the Large-scale Circulation

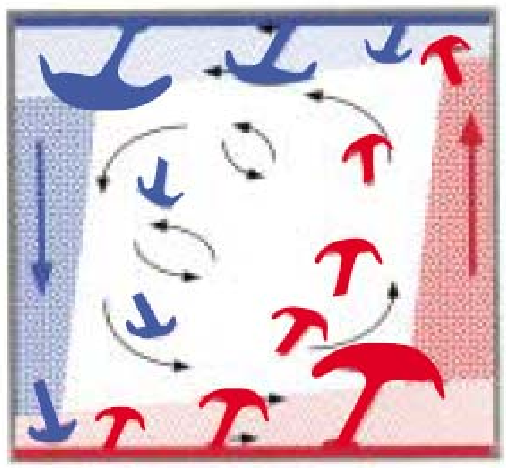

Kadanoff, *Physics Today* (2001)

- A large-scale-circulation (LSC) exists in RB system
- Cioni et al observed azimuthal rotation of the LSC in mercury convection (*JFM 1997*).
- Niemela et al found reversals of LSC in helium (*JFM 2001*).

Flow reversal occurs in many turbulent flow systems.

Reversal of the LSC in turbulent convection may be related to natural phenomena such as the reversal of the geomagnetic polarity.

Reversal phenomenon

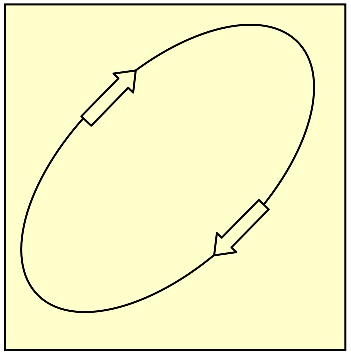

Two scenarios → In-plane reversal

→ 180^o azimuthal rotation

Statistical analysis and physical models:

Sreenivasan, Bershadskii and Niemela, *PRE 2002*, *Physica A 2004*, *Physics Lett. 2004*, *Hwa et al*, *PRE 2005*

Benzi, *PRL 2005*.
Araujo, Grossmann and Lohse, *PRL 2005*.

More recent experiments:

Brown, Nikolaenko & Ahlers, *PRL 2005;* Brown & Ahlers, JFM 2006
Sun, Xi & Xia, PRL 2005, Xi, Zhou, & Xia (PRE 2006)

Ahlers group found both the in-plane reversal and 180^o azimuthal rotation can occur and identified the 'cessation' phenomenon.

Xia group found the azimuthal motion of LSC plane consists of net rotations and erratic fluctuations. The residents phenomenon is observed.

Motivation

- The physical pictures in theoretical models appear to apply to unity aspect ratio geometry.

- Can cessations occur in small aspect ratio geometry ?

- What happens to the LSC during a cessation?

The PIV measurement

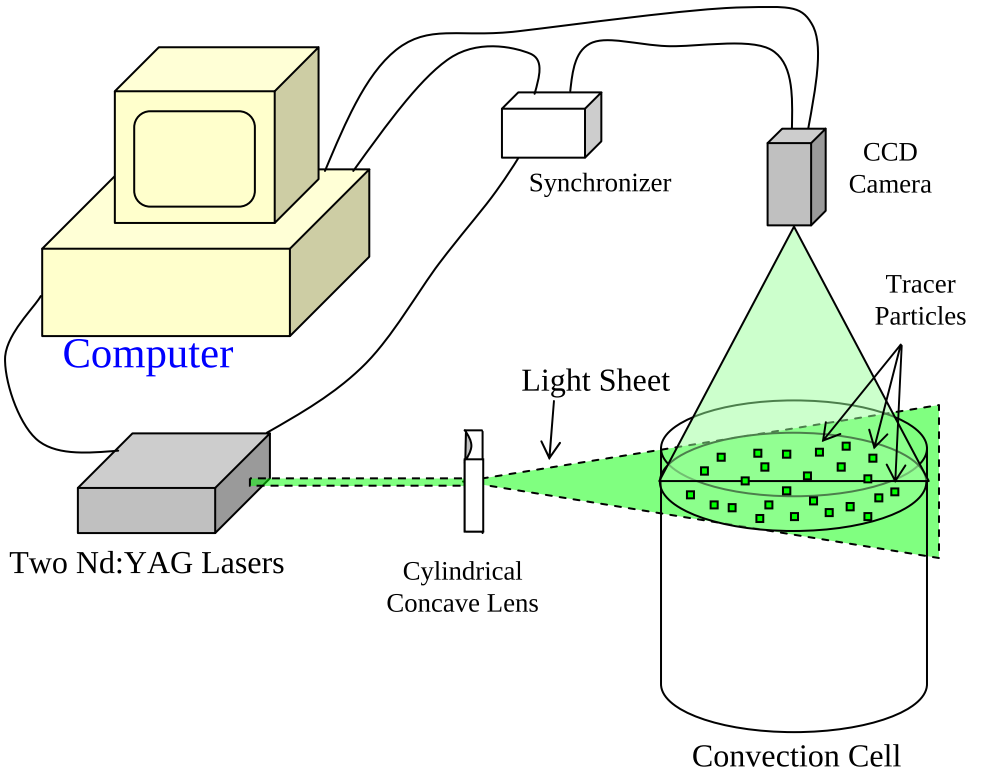

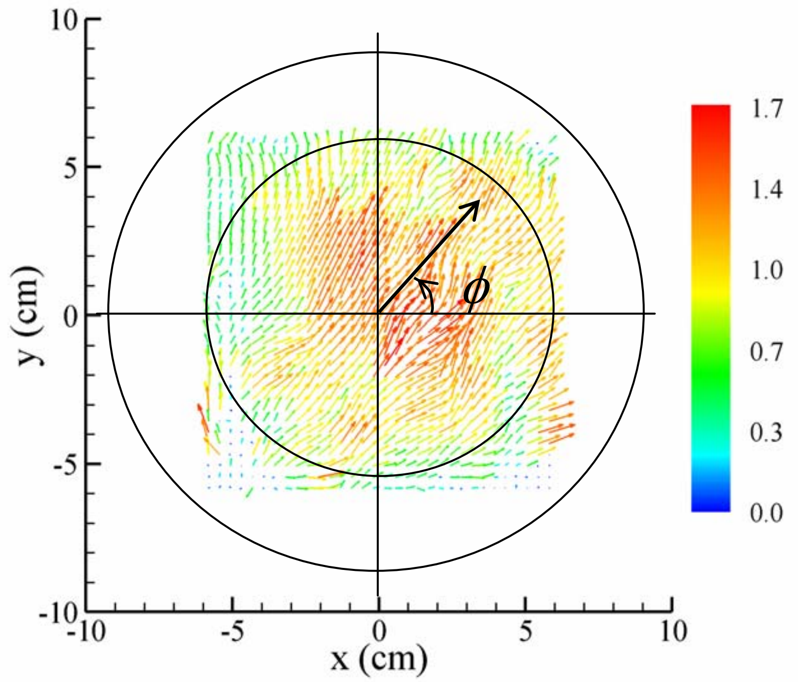

Xi, Zhou and Xia, *PRE* (2006)

The Multi-thermistor measurement

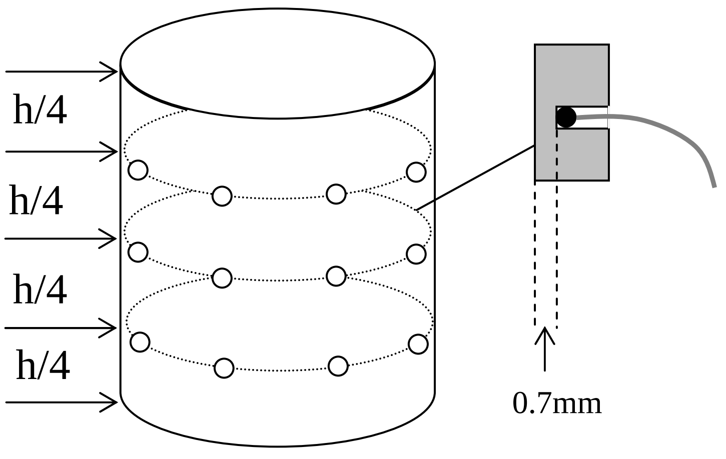

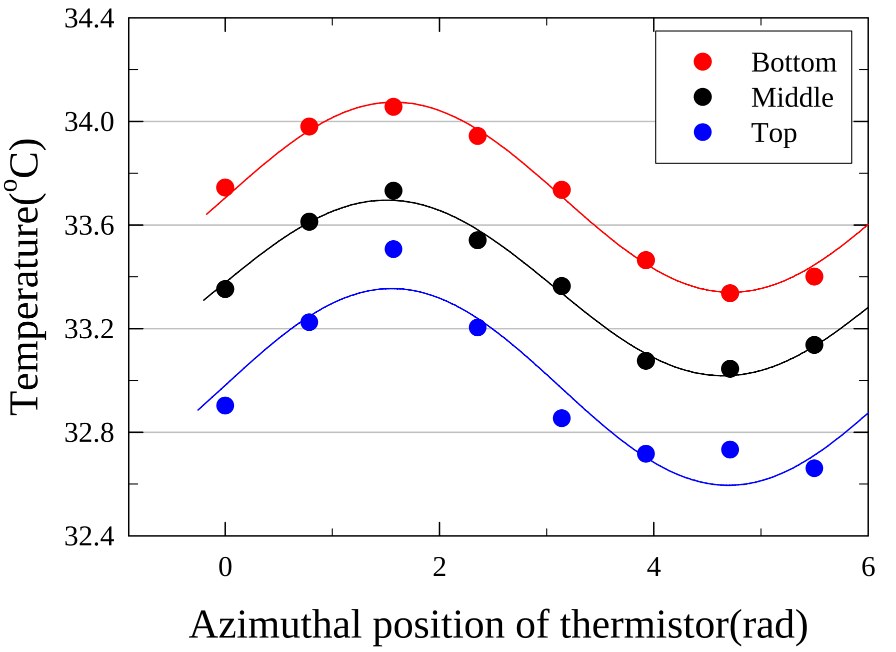

$$T_i = T_0 + A\cos(i\pi/4 - \phi)$$

A(t) measures the flow strength (amplitude of the LSC)
ϕ(t) is the azimuthal postion where the hot side of the LSC goes up.

Brown, Nikolaenko, and Ahlers (*PRL 2005)*

Cessations in $\Gamma = ½$ convection cell

Setup and parameter range:

Sapphire cell

- **PIV, Multi-thermistor simultaneously**

  $Ra = 5.7\times10^{9}$, 1.5×10^{10}, 3.3×10^{10}, $Pr = 5.3$

- **Multi-thermistor**

  $Ra = 1.4\times10^{10}$, 1.5×10^{10}, 1.6×10^{10}, 3.0×10^{10}, 3.3×10^{10}, 4.3×10^{10}, 7.2×10^{10}

  $Pr = 4.9\text{-}5.3$

Copper cell

- **Multi-thermistor, 34-day measurement. $Ra = 5.6\times10^{10}$**

The same statistical results are obtained from all these measurements

The examples of cessation in Γ = ½ cell

PIV result

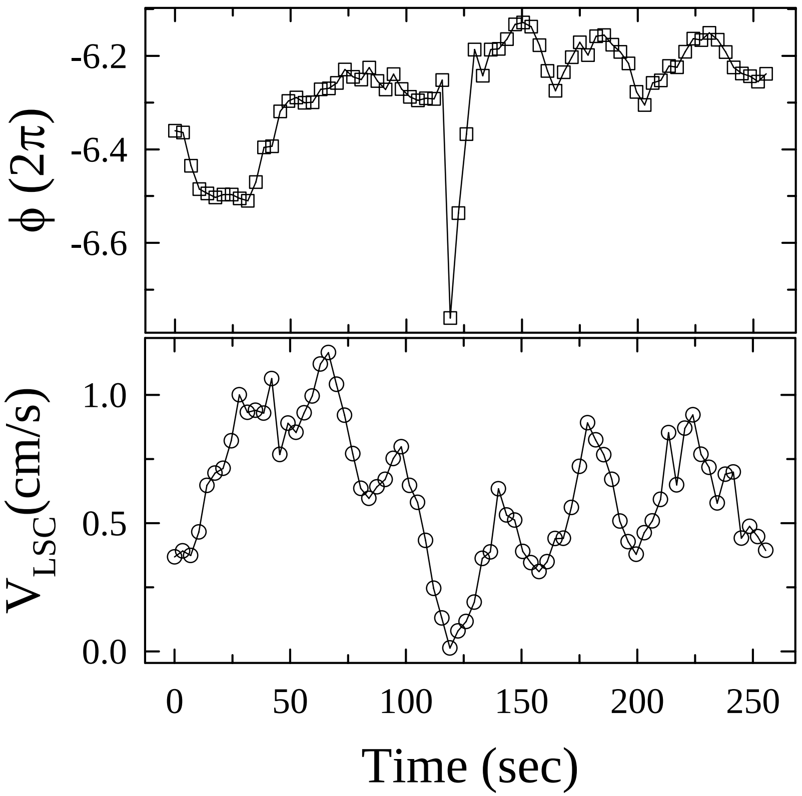

Muti-thermistor result

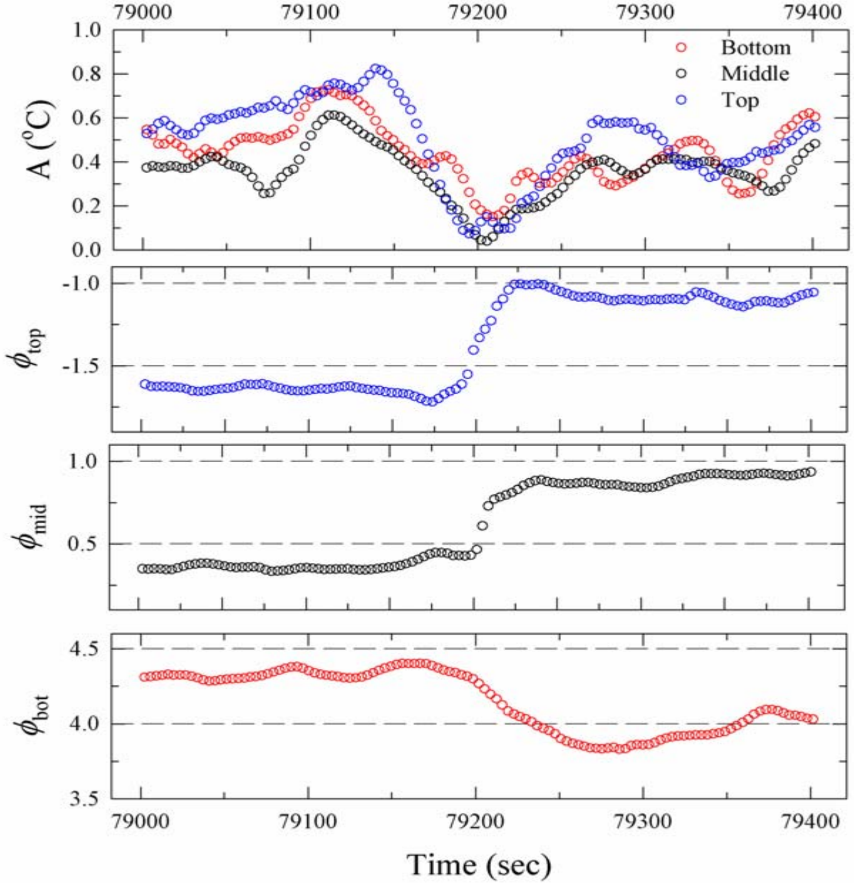

The definition of a cessation

Cessation is defined by $V_{LSC} < (V_{LSC})_l$

Duration τ_d of cessation is defined by $V_{LSC} < (V_{LSC})_h$

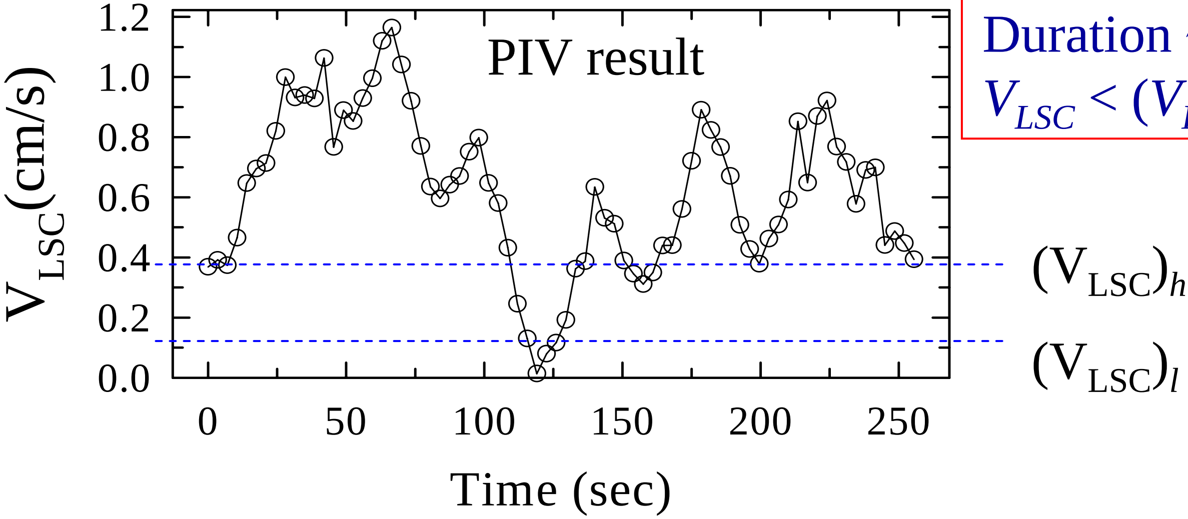

$(V_{LSC})_l = 0.1 \langle V_{LSC} \rangle$

$(V_{LSC})_h = 0.3 \langle V_{LSC} \rangle$

Cessation is defined by $A < (A)_l$

Duration of cessation τ_d is defined by $A < (A)_h$

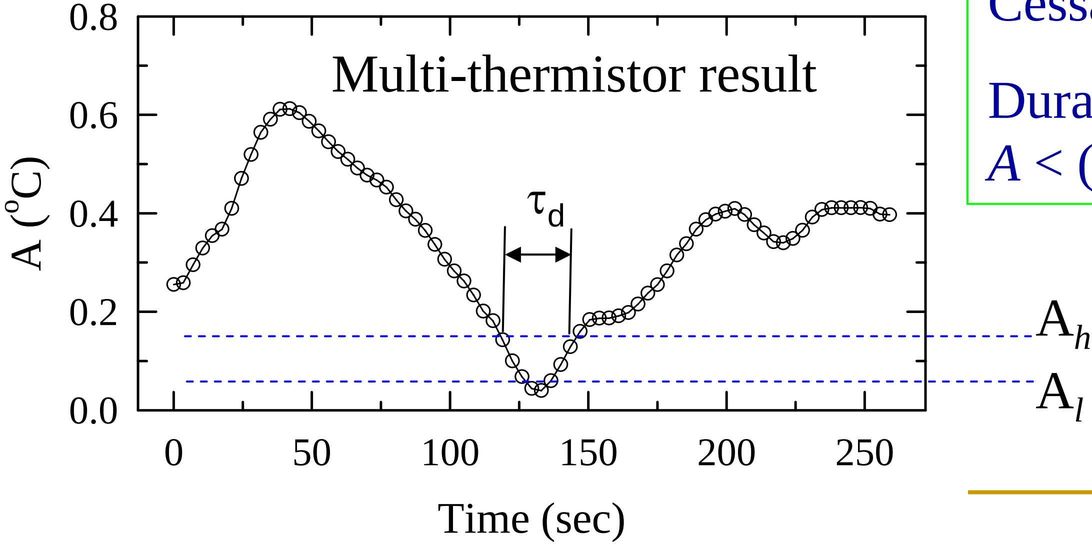

$A_l = 0.1 \langle A \rangle$

$A_h = 0.3 \langle A \rangle$

Thresholds explored

$(V_{LSC})_l = (0.05 \sim 0.2)\langle V_{LSC} \rangle$

$(V_{LSC})_h = (0.2 \sim 0.8)\langle V_{LSC} \rangle$

Similar statistics are obtained

$A_l = (0.05 \sim 0.2)\langle A \rangle$

$A_h = (0.2 \sim 0.8)\langle A \rangle$

Similar statistics are obtained

- PIV, multi-Ra: **466** cessations
- Multi-thermistor, multi-Ra: **1778** cessations
- Single-Ra, 34-day measurement: **1071** cessations

All give similar statistics

The number of cessations identified by the 3 rows of thermistors at different heights differ by less than 3%, and the statistics are all the same.

Examples of cessations, multi-thermistor (middle height)

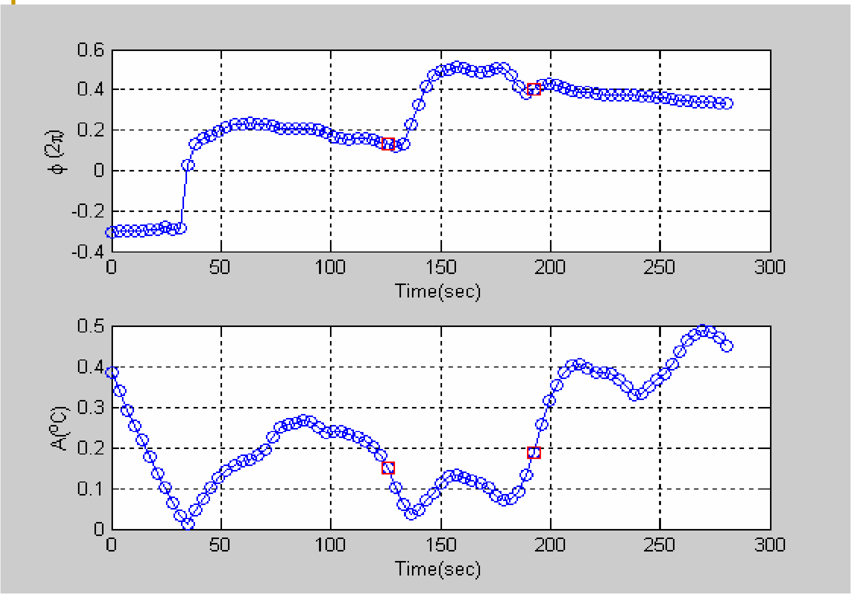

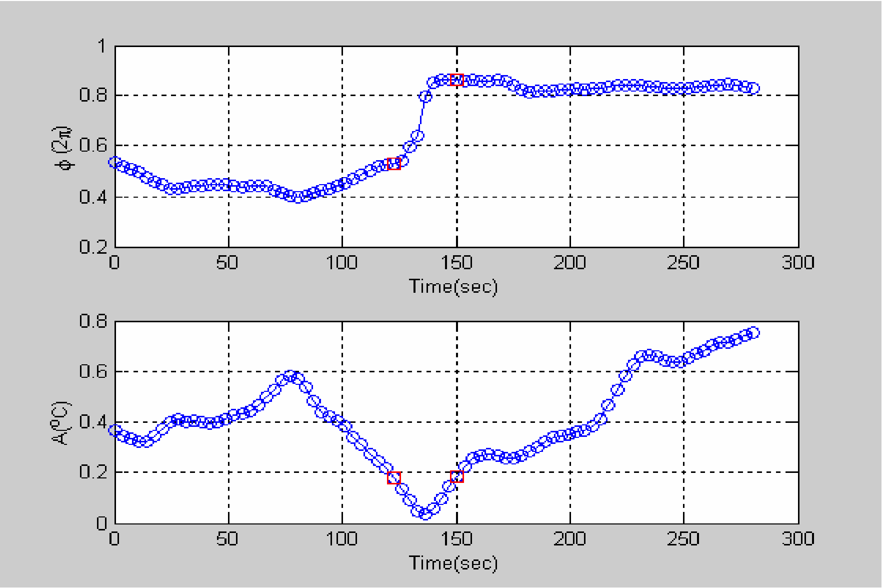

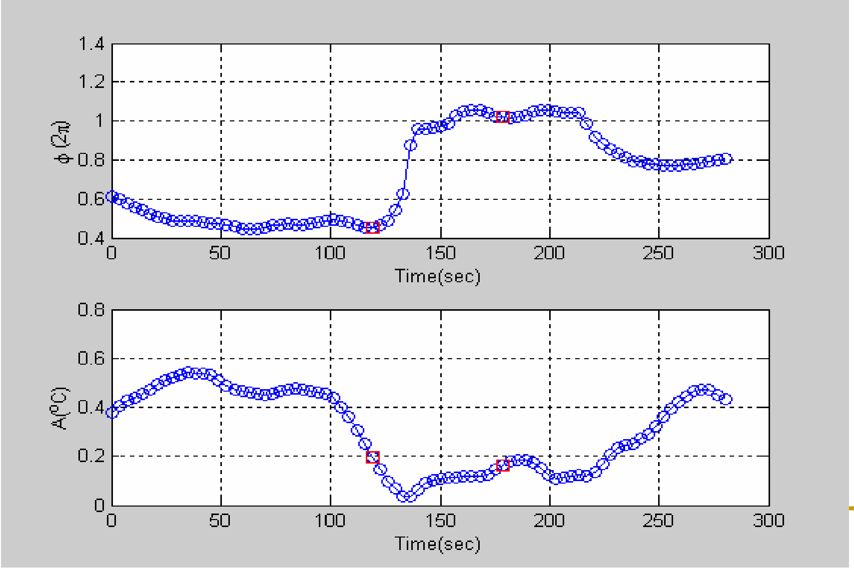

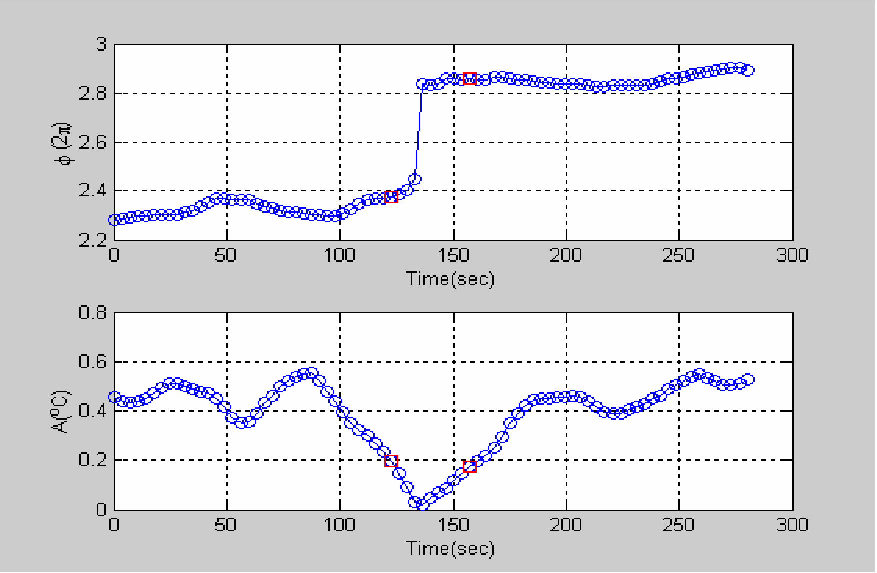

Examples of cessations, multi-thermistor (bottom row)

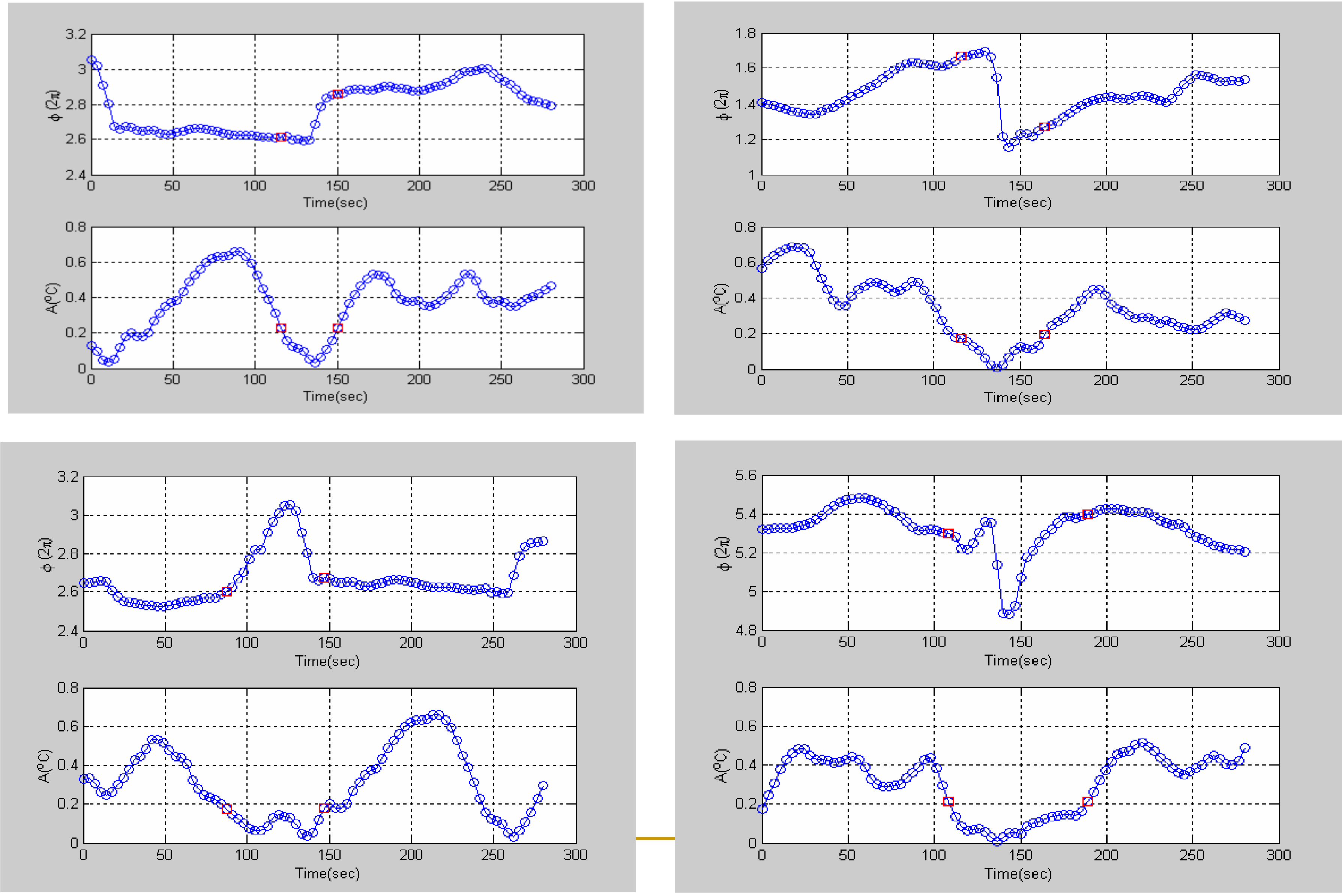

PIV result

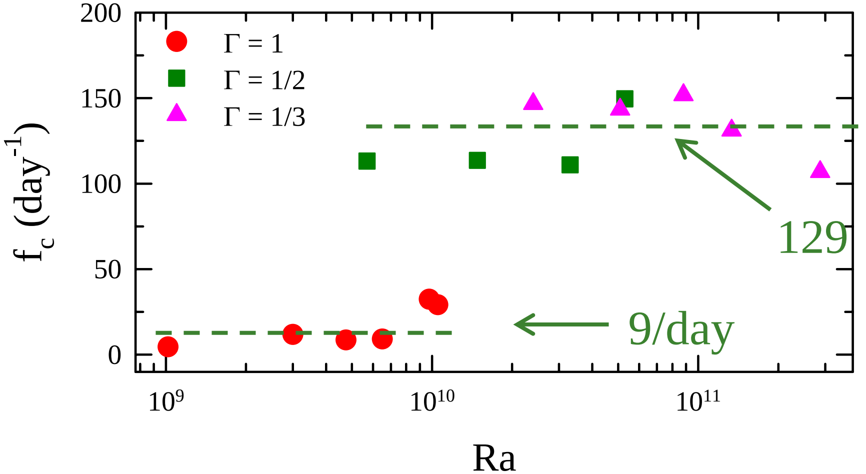

$$\frac{f_c(\Gamma = 1/2,\ 1/3)}{f_c(\Gamma = 1)} = 14$$

$$f_c(PIV)/\ f_c(therm) = 3.7 \sim 6$$

Γ = 1 PIV data is reanalyzed using new definition (96 now vs. 28 in Xi et al, PRE 2006)

Multi-thermistor result

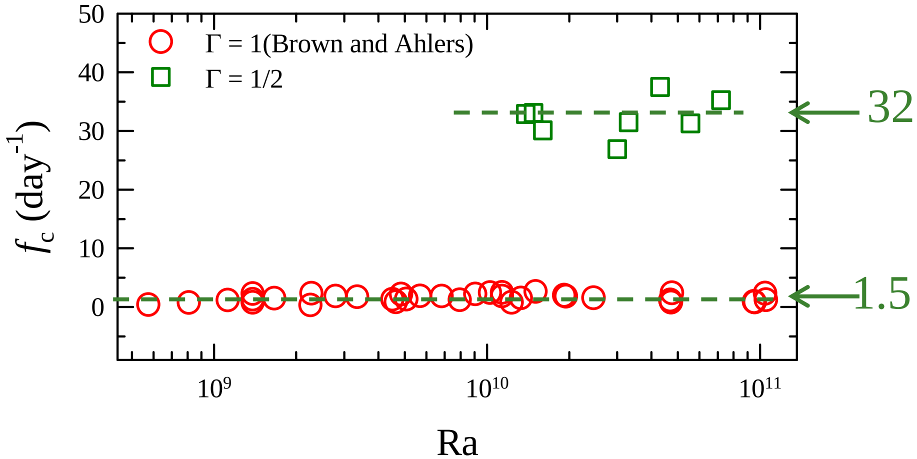

$$\frac{f_c(\Gamma = 1/2)}{f_c(\Gamma = 1)} = 20$$

Cessations in $\Gamma < 1$ cells occur an order of magnitude more frequent than in $\Gamma = 1$ cells.

Brown and Ahlers, JFM 2006

Orientational change $\Delta\phi$ of LSC before and after a cessation

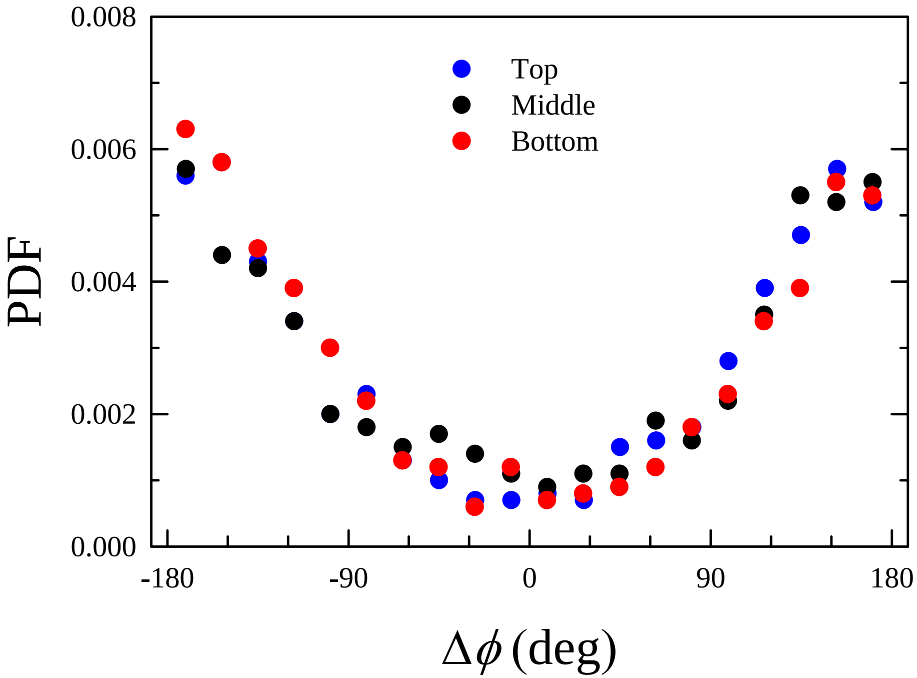

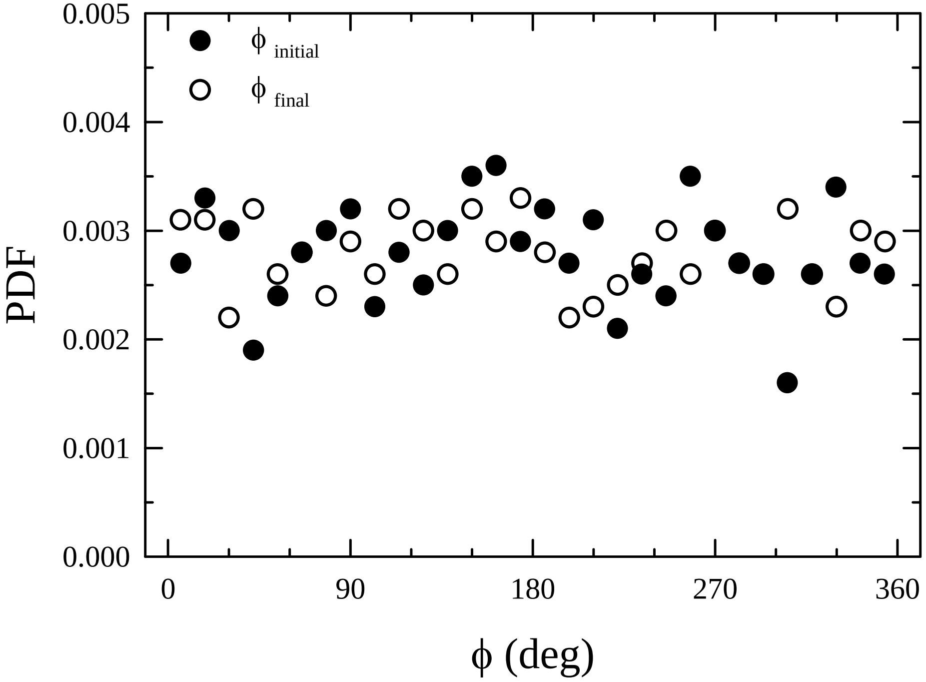

Uniform distribution in $\Gamma = 1$ cell (Brown and Ahlers, PRL05, JFM 2006; Xi, et al PRE 2006)

$\phi_{initial}$ and ϕ_{final} --- orientation of LSC before and after a cessation

Cessations with $|\Delta\phi|$ close to 180 is 6 times more likely to occur than cessations with small $|\Delta\phi|$

Statistics of cessation

Cessation statistics in $\Gamma=1/2$ are similar to the $\Gamma=1$ case, except that of $\Delta\phi$

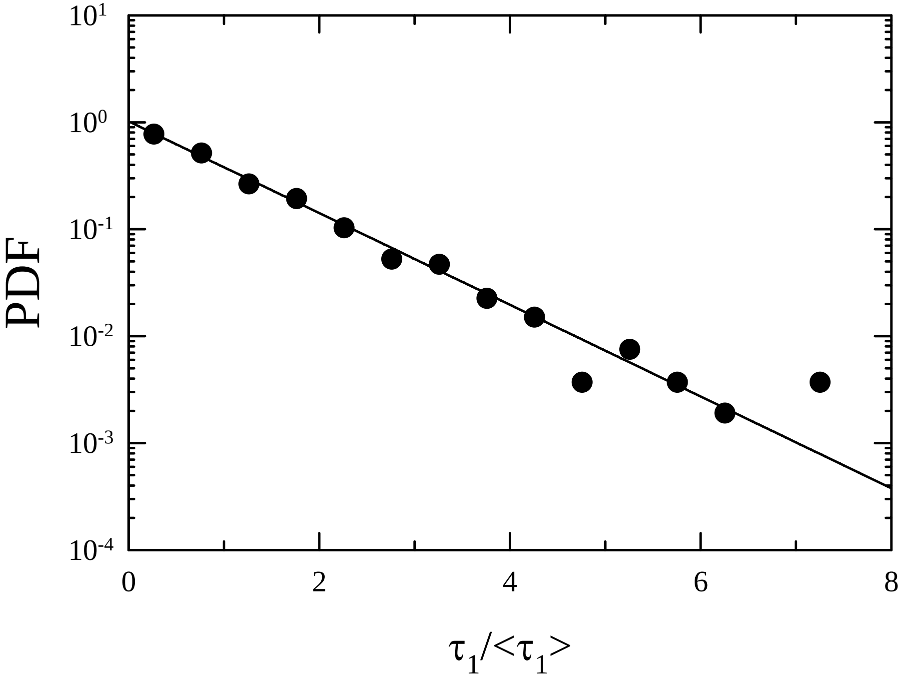

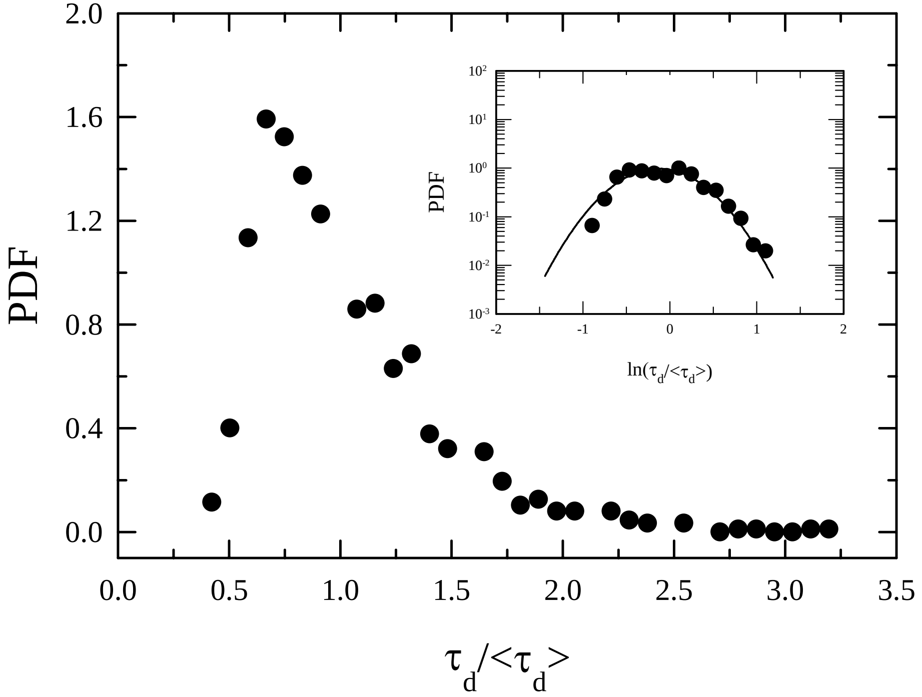

τ_1 ---- time between successive cessations.

The straight line is: $p(\tau_1/<\tau_1>) = \exp(-\tau_1/<\tau_1>)$

τ_d --- duration of a cessation

$<\tau_d>$ = 46 s, max = 150 s, min = 18 s

$<\tau_1>$ = 46 min., $<\tau_1>_{max}$= 342 min, $<\tau_1>_{min}$= 0.7 min

Benzi, PRL, 2005; Brown and Ahlers , JFM 2006.

Statistics of cessation

t_n --- the time that nth cessation occurs

The PDF and power spectrum of detrended t_n.

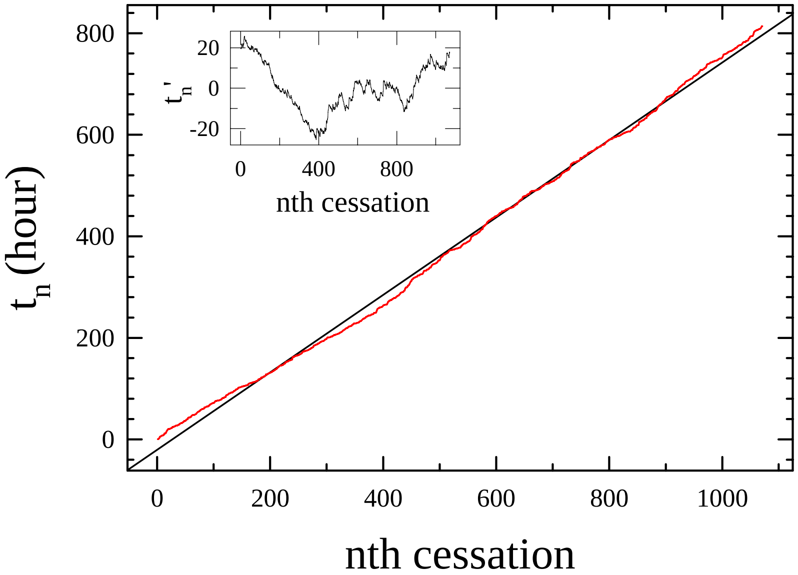

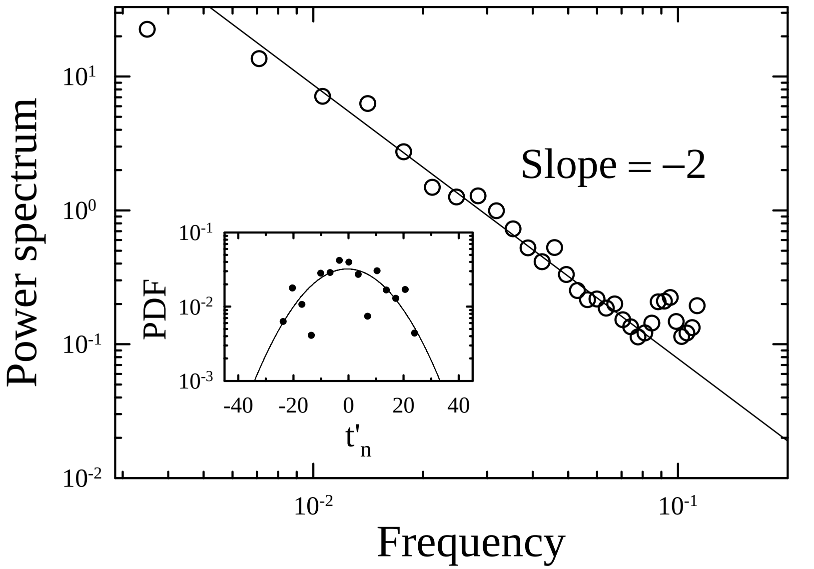

The statistics for t_n are consistent with those of "reversals" found by Sreenivasan, Bershadskii and Niemela (PRE2002), and "crossings" by Xi, Zhou and Xia (PRE2006) . But not those for τ_1 (no power law for small τ_1).

What happens during the cessation?

$\Gamma = 1$

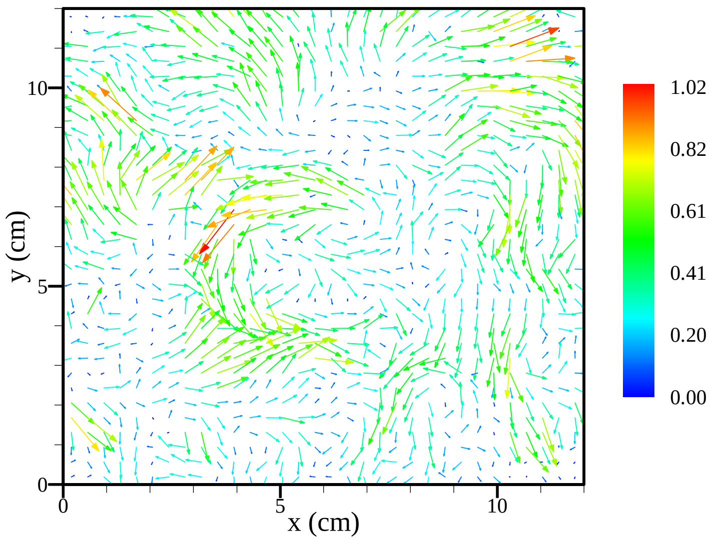

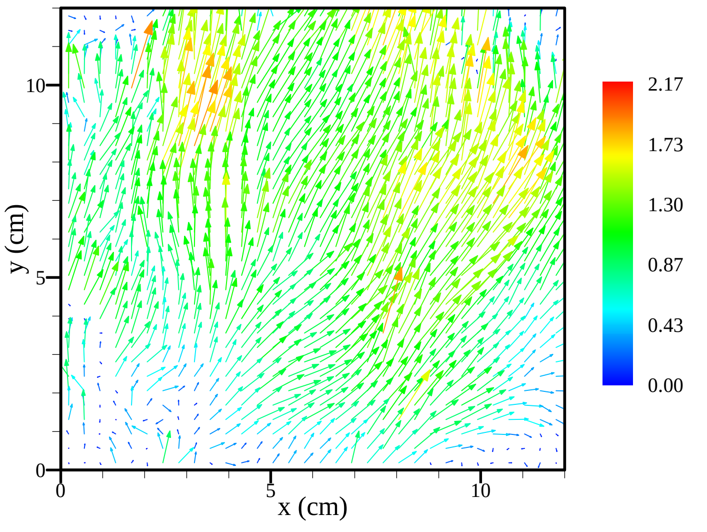

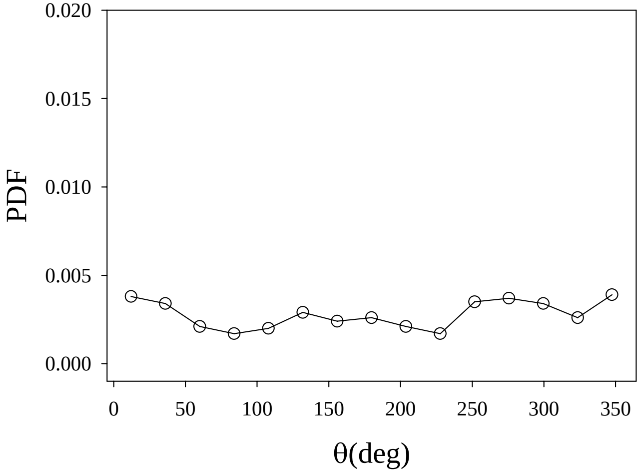

Incoherent mean wind

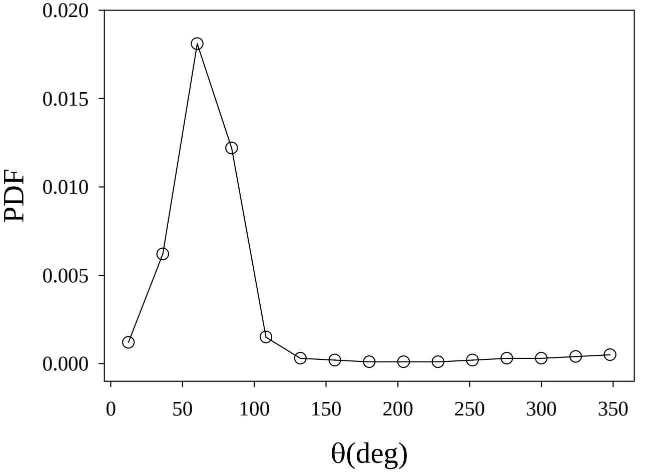

coherent mean wind

What happens during the cessation?

$\Gamma = 1/2$

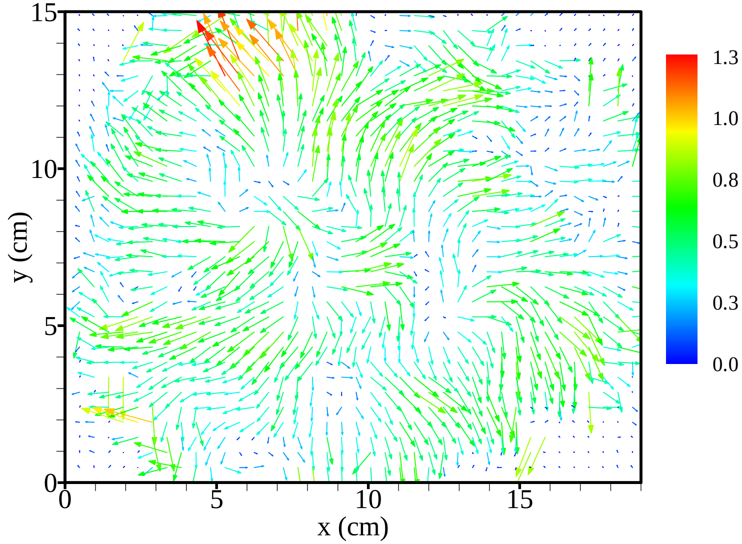

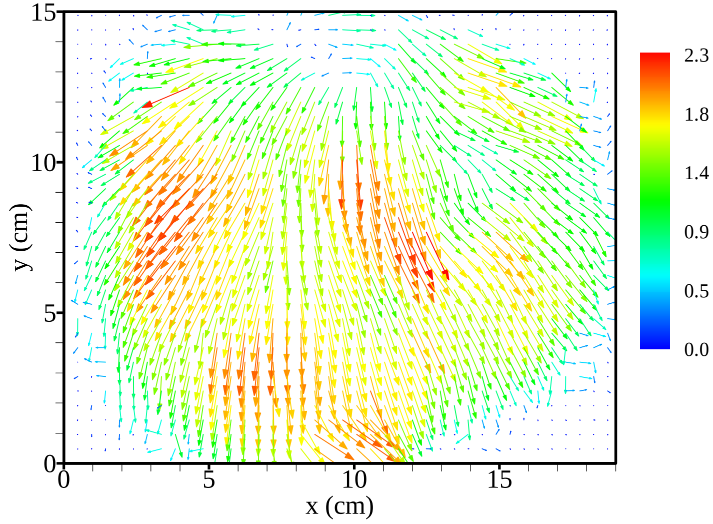

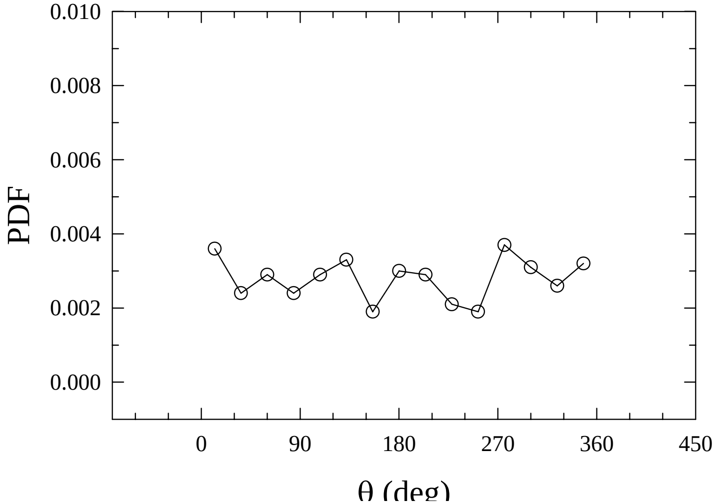

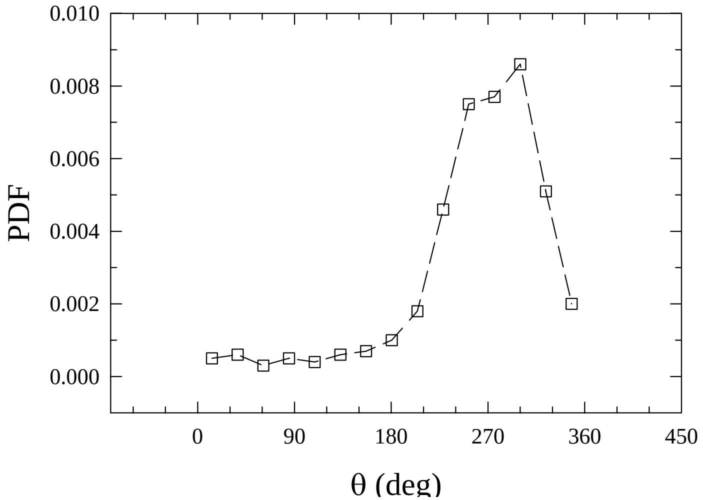

Incoherent mean wind

coherent mean wind

Three incoherent modes causing cessations

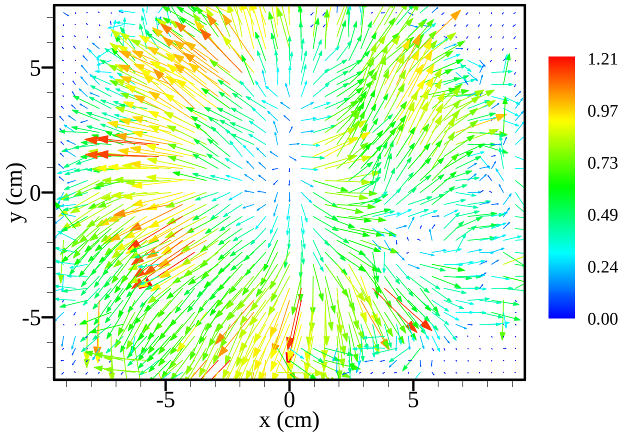

Incoherent flow, radial mode

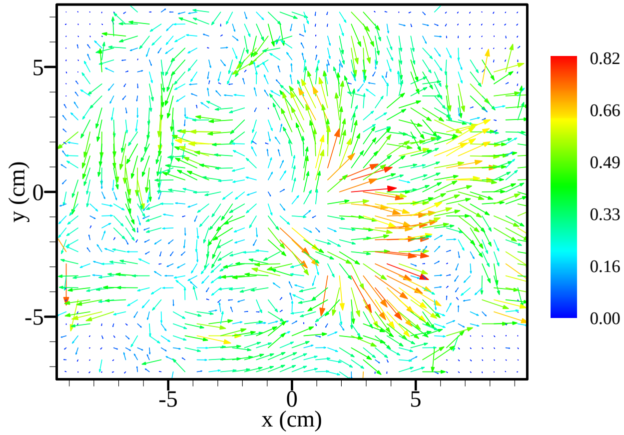

Incoherent flow, chaotic mode

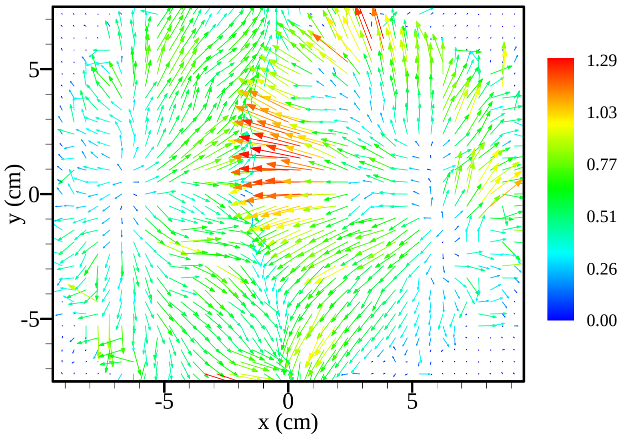

Incoherent flow, competing mode

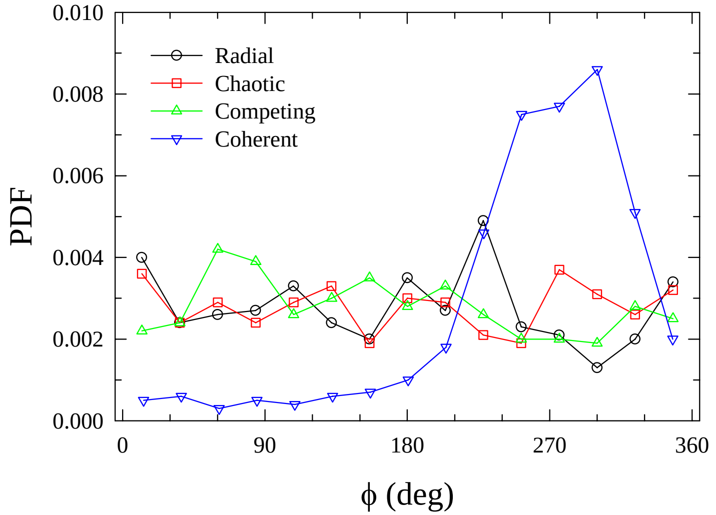

The measured time trace of orientation of LSC plane

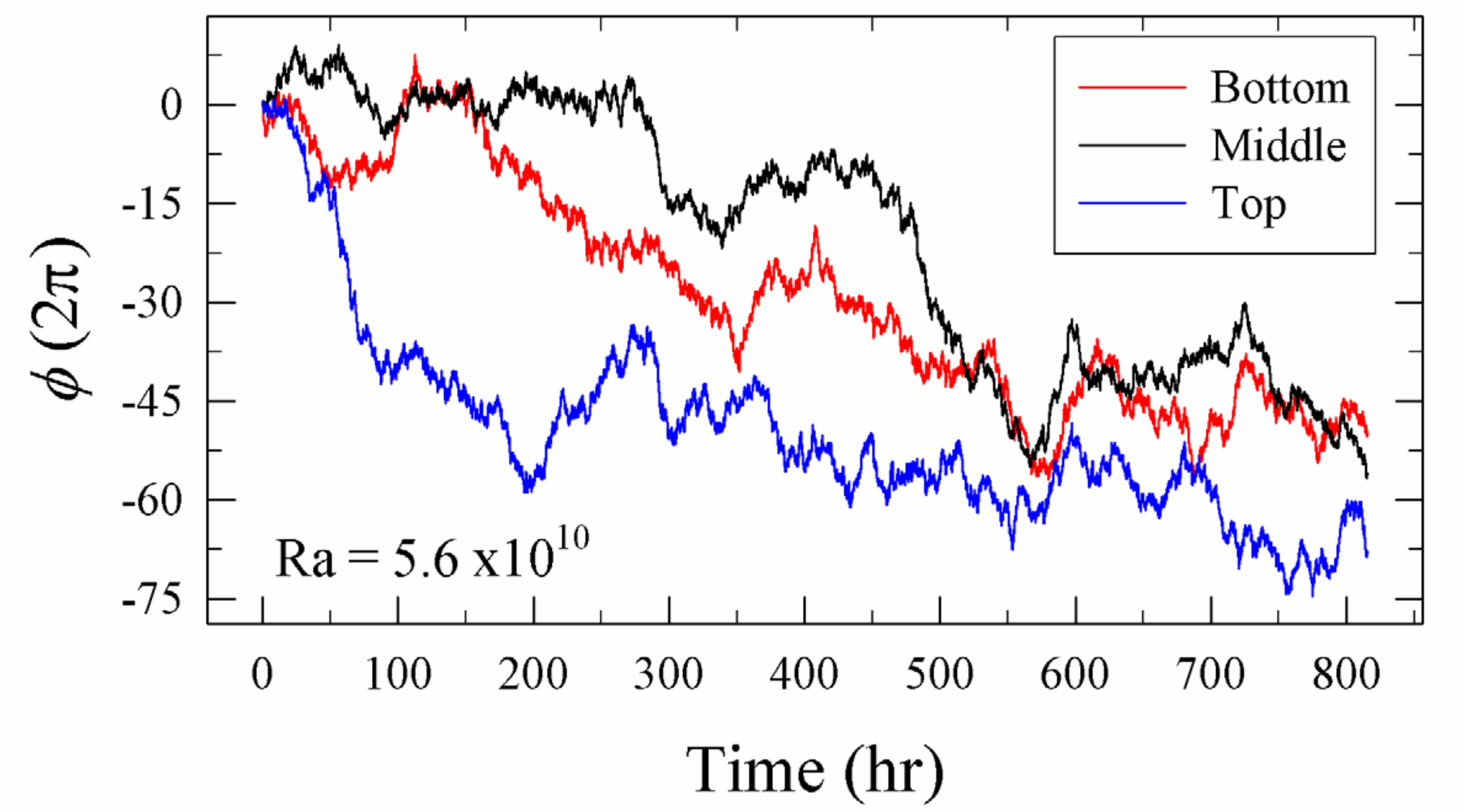

Positive is counterclockwise

Possible scenario for the divergence of ϕ obtained at different heights

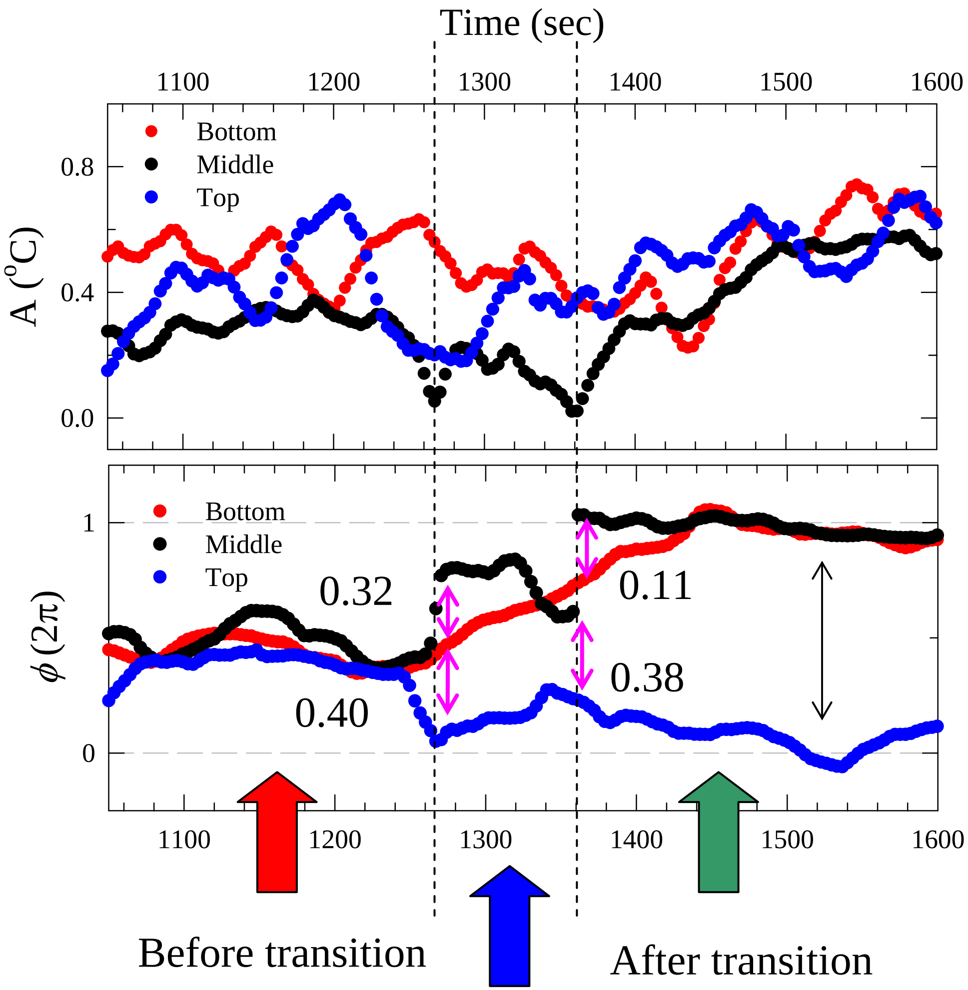

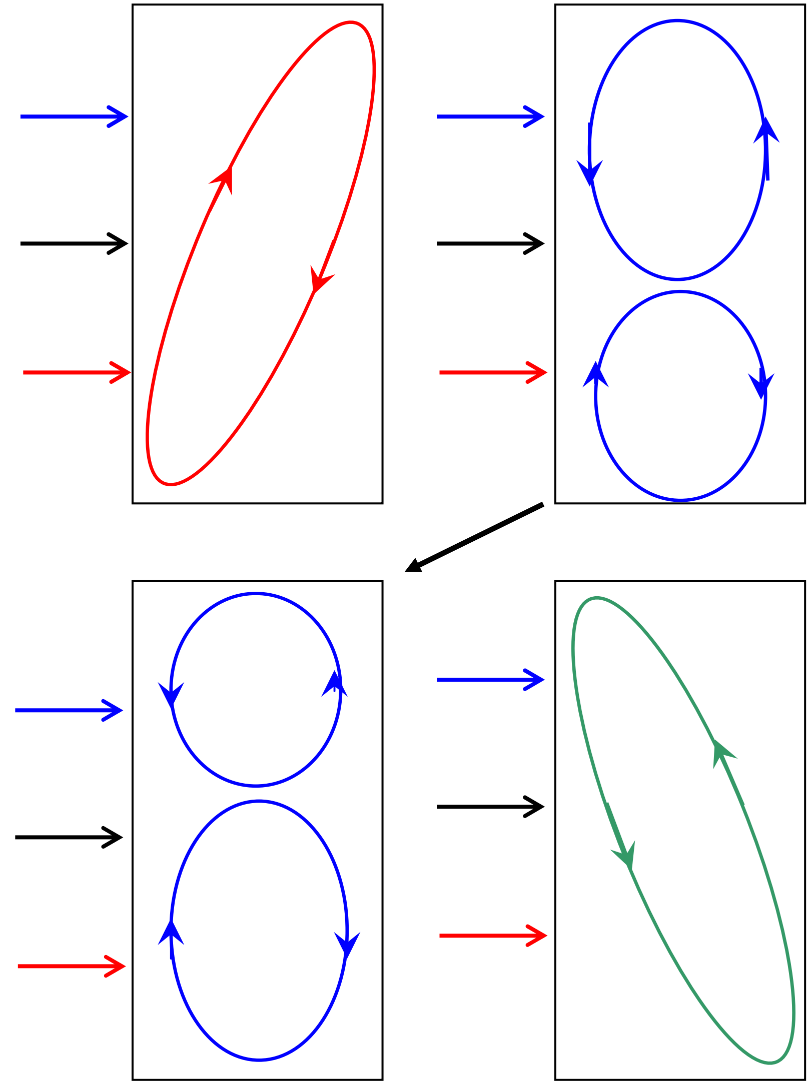

Flow mode transition between dominant and minor modes

Verzicco and Camussi, (JFM 2003)

More examples of flow-mode transitions

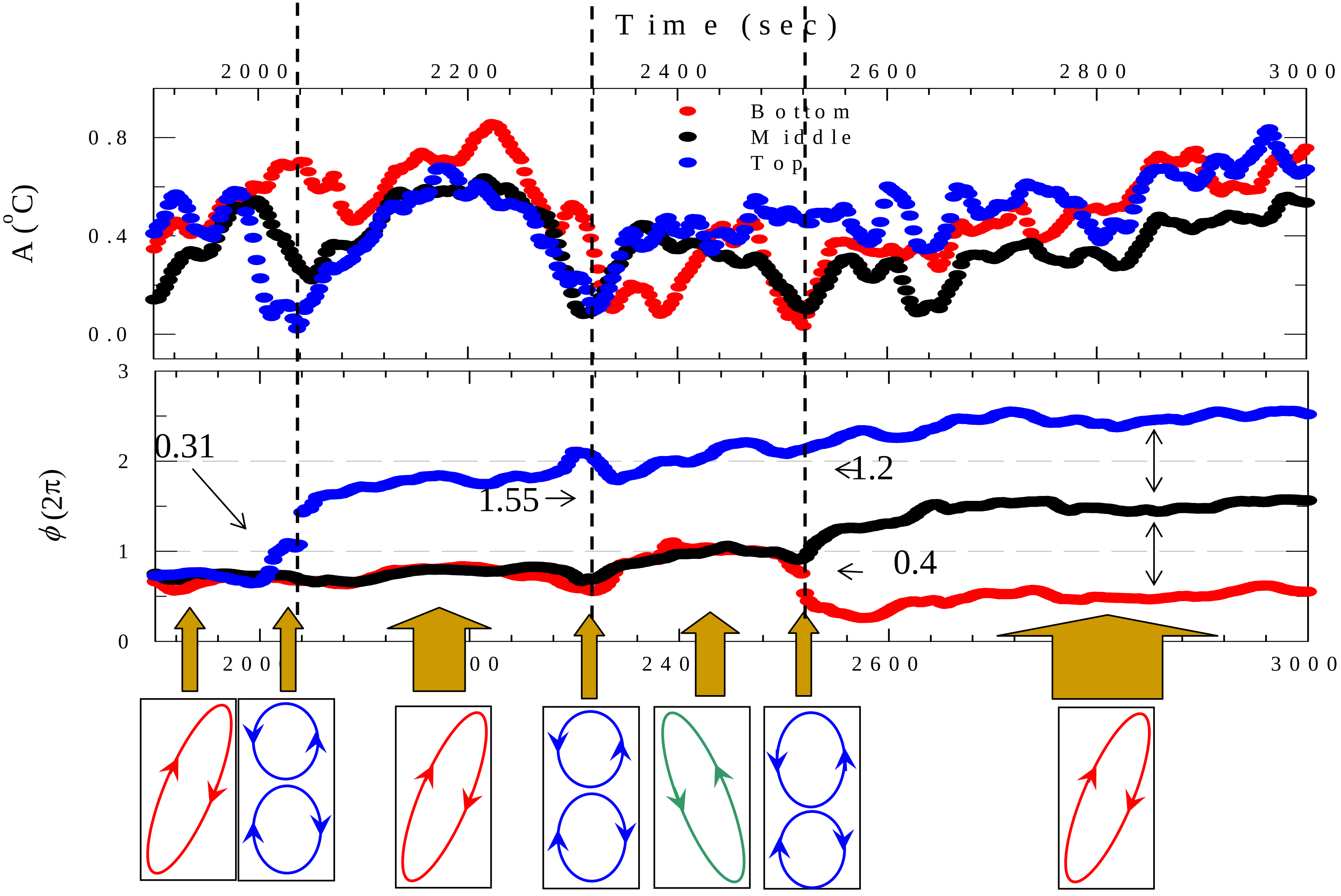

Duration of flow mode transition is less than 100 second.

The orientation trace in cells of different Γ

PIV result

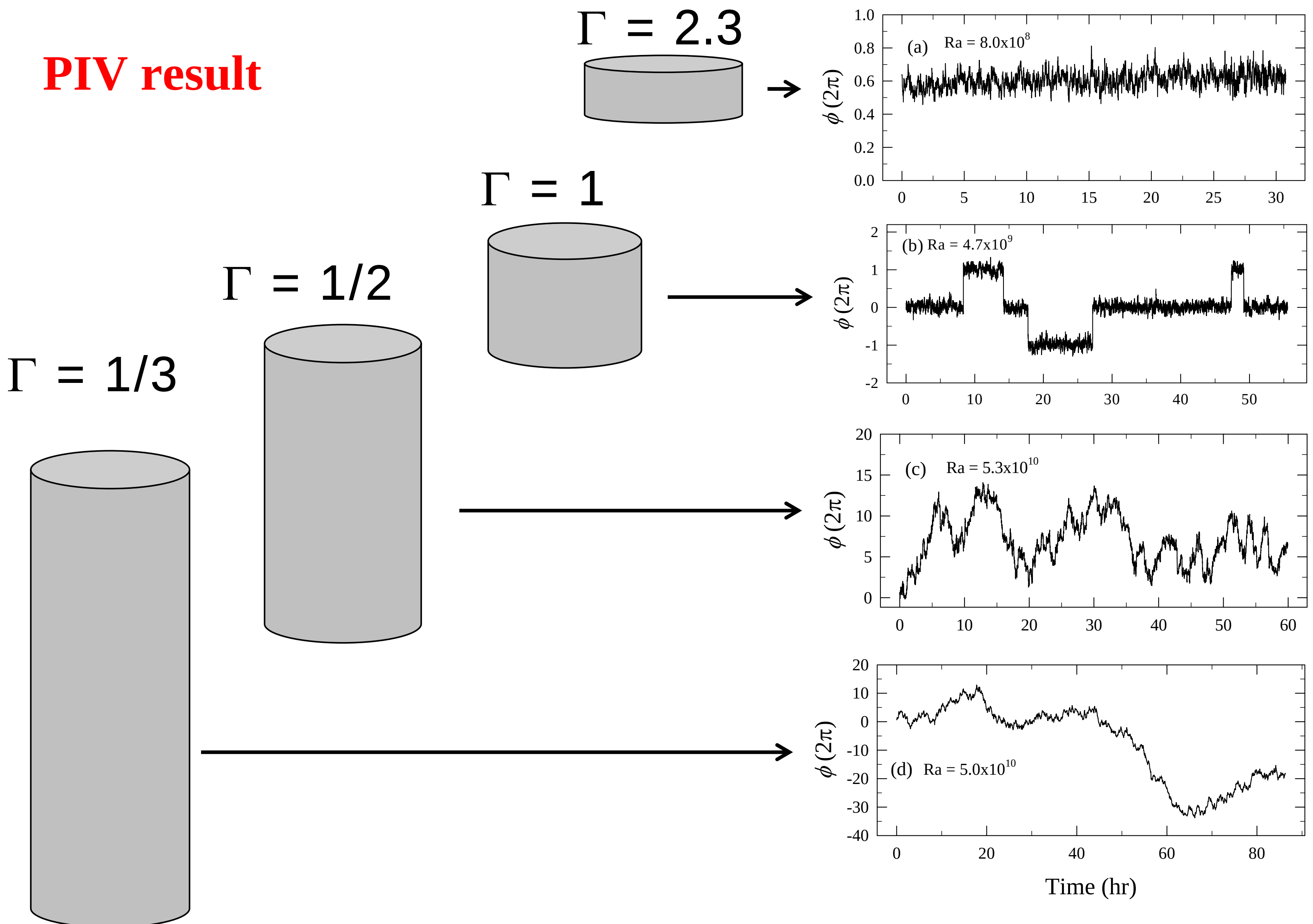

The plots of the traces in polar coordinate

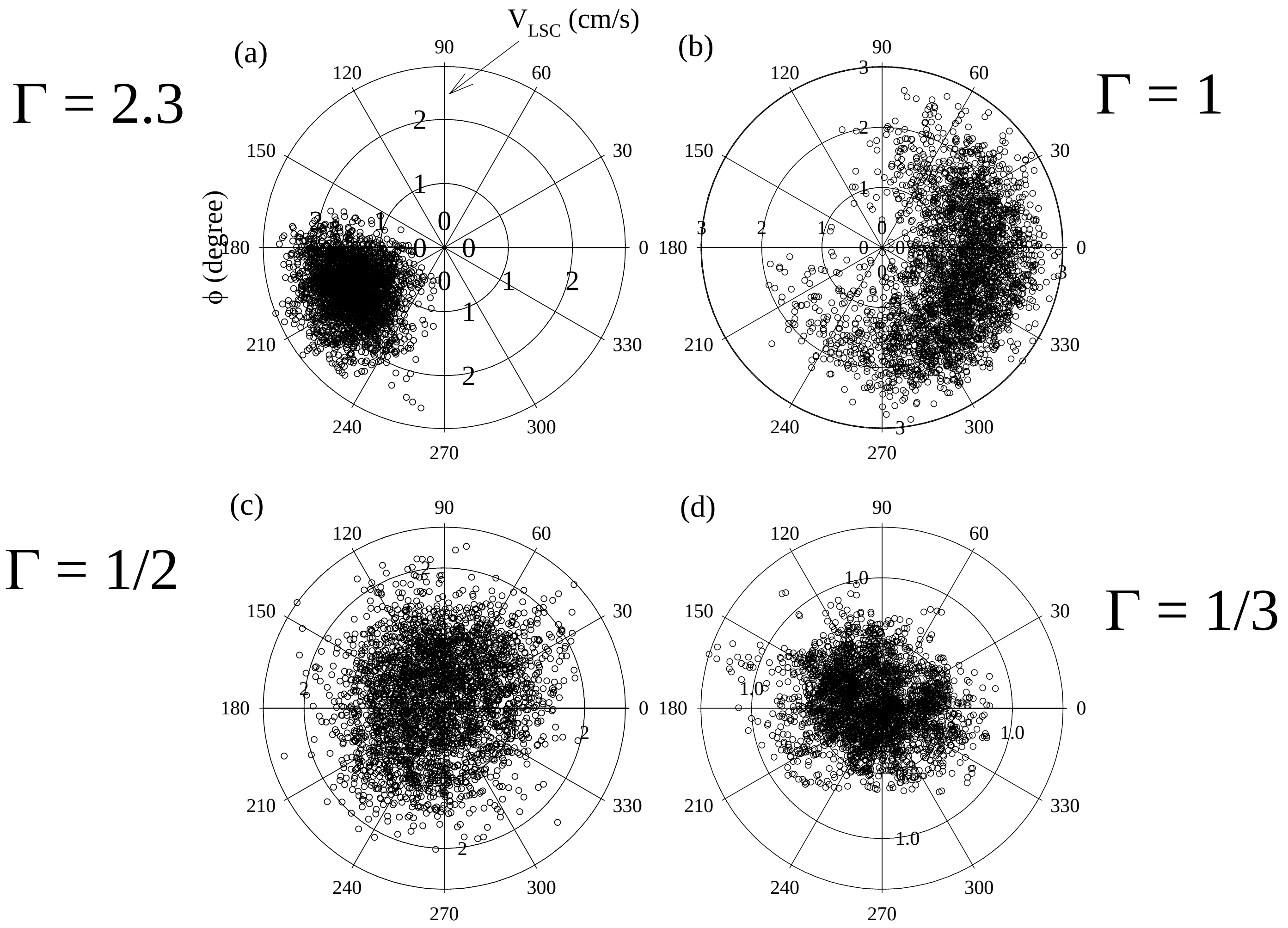

The PDF of the orientation of LSC for different aspect ratio

PIV sapphire cell

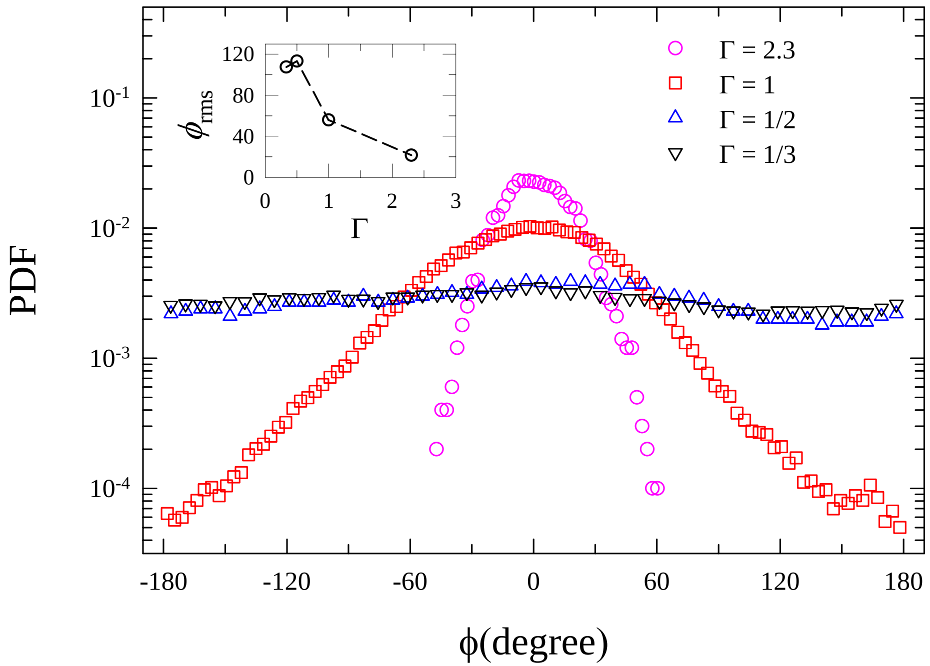

Multi-thermistor result

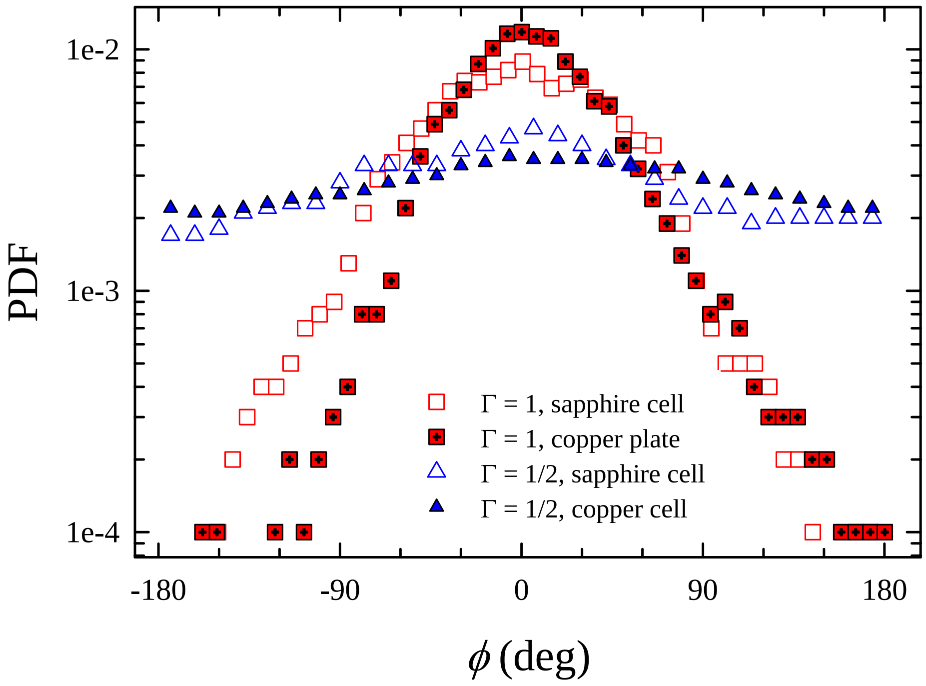

Summary of Part 2

- Cessations occur an order of magnitude more frequently in small Γ cells than in cell with Γ =1. The frequency of occurrence has no obvious dependence on Ra.
- The LSC likes to reverse its direction after a cessation in cells with Γ =1/2.
- Common features of the statistics properties based on pure-cessation events, rotations/reorientations, reversals, and crossings suggest that all these phenomena may share the same origin.
- Constraints for theoretical models (SOC, dynamical systems, stochastic).
- A cessation event is a process of de-coherence, or disorganization and reorganization of the LSC.
- Flow-mode transitions may have been observed indirectly by temperature measurement.

Part 3

Morphological evolution and geometrical properties of turbulent thermal plumes

Mushroom-like Plumes

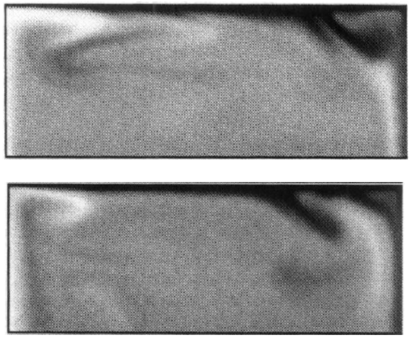

Werne (1994)

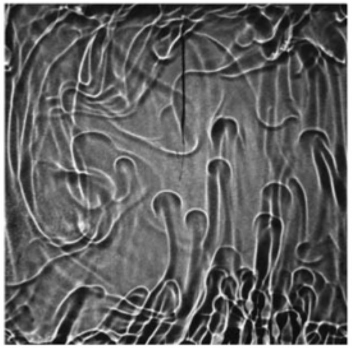

Zhang, Childress, Libchaber (1997)

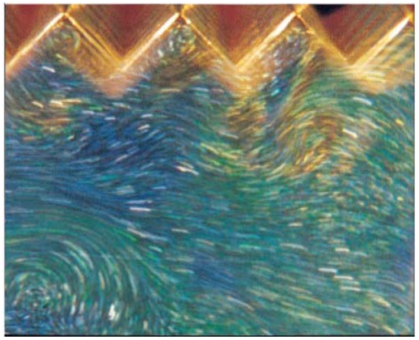

Du & Tong (1998)

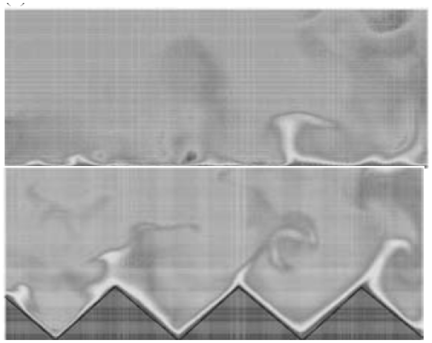

Stringano, Pascazio & Verzicco (2006)

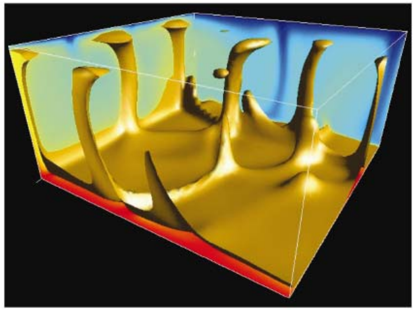

Breuer, Wessling, Schmalzl & Hansen (2004)

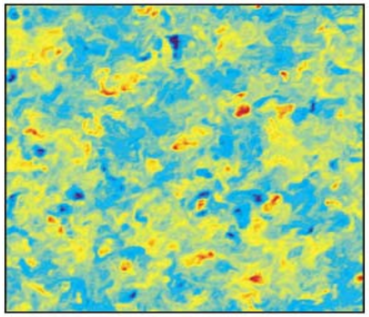

Parodi et al. (2004)

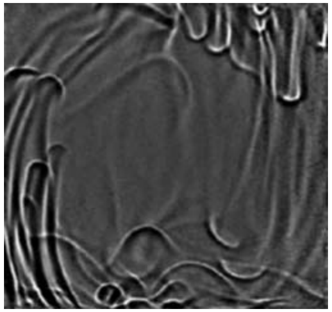

Xi, Lam & K.-Q. Xia (2004)

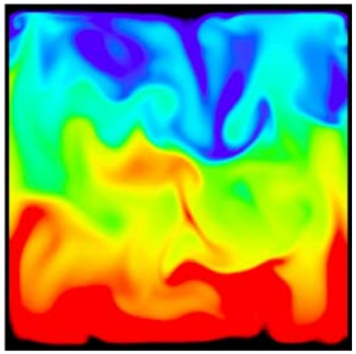

Toschi (2006)

Sheet-like Plumes

Zocchi, Moses, Libchaber (1990)

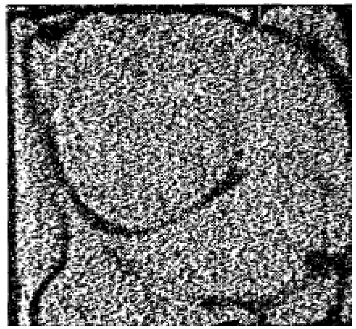

Gluchman, Willaime, Gollub (1993)

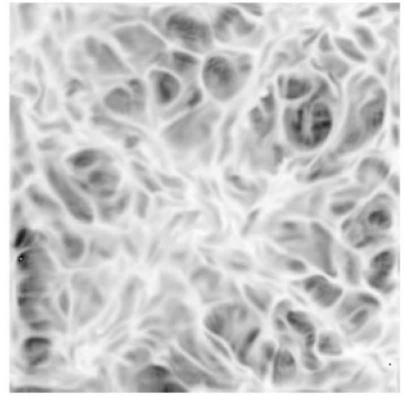

Kerr (1996,2000)

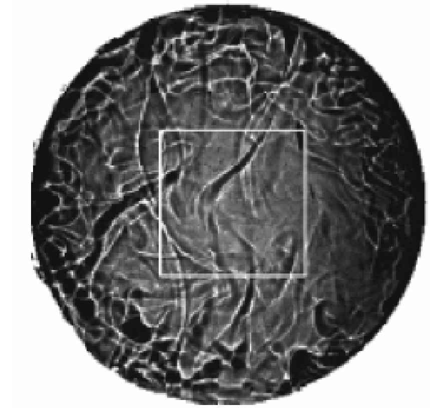

Funfschilling & Ahlers (2004)

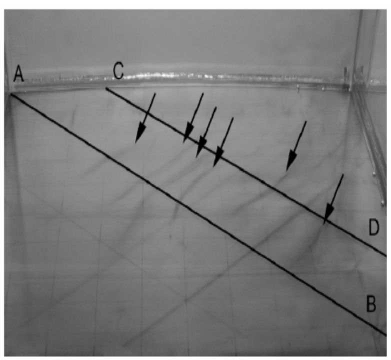

String-like coherent structure

Haramina and Tilgner (2004)

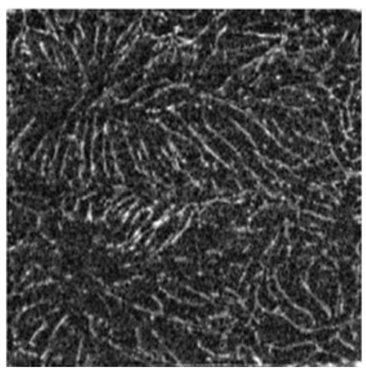

Puthenveettil & Arakeri (2005)

?

Sheet-like plumes → **Mush-like plumes**

Motivation

What are the geometrical and thermal properties of the plumes as individual objects?

How do sheet-like plumes transform into mush-like ones?

This work represents the an attempt to quantitatively characterize these coherent structures, which remain largely unexplored.

Experimental setup

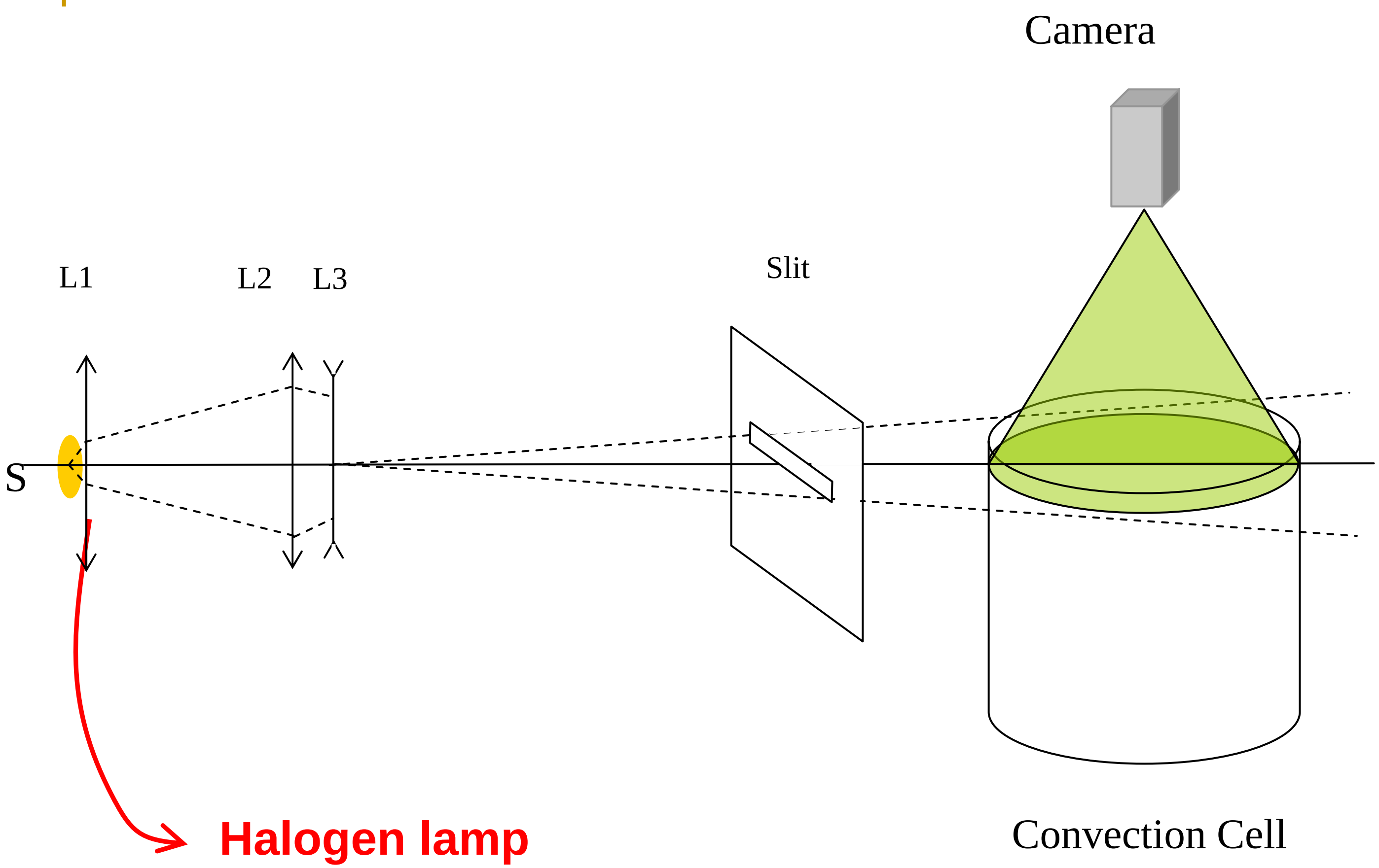

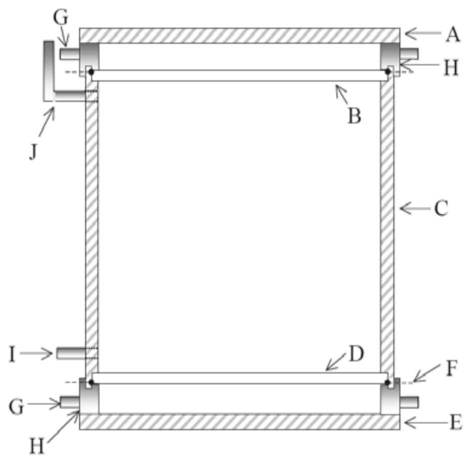

TLC: Thermochromic liquid crystal microspheres (R29C4W), 50 μm mean diameter.

Red: 29-29.5^{o}C;   Green: 29.5-29.7^{o}C;   Blue:29.7-33^{o}C

Zocchi, Moses & Libchaber (1990); Gluchman, Willaime & Gollub (1993); Du & Tong (1998)

Sheet like plumes

3 mm from top plate

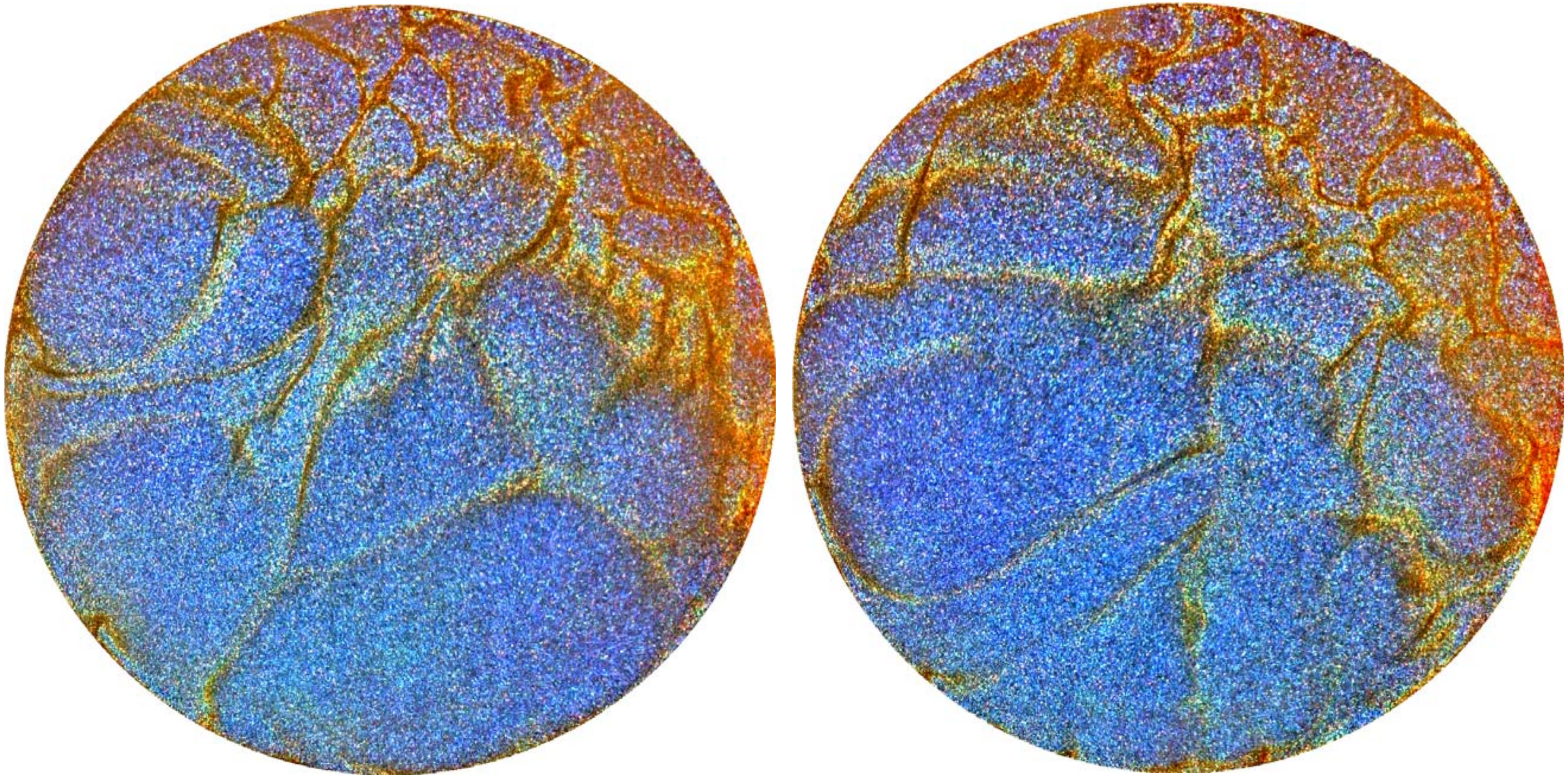

Sheet like plumes were observed near boundary layer.

Extraction of sheet-like plumes

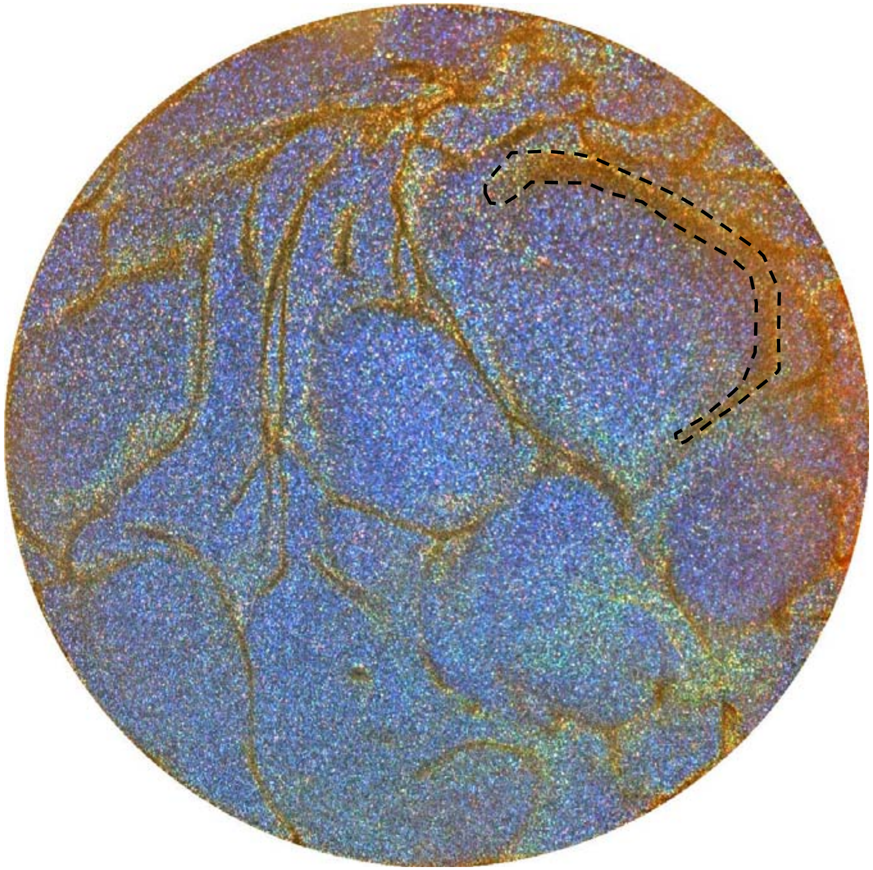

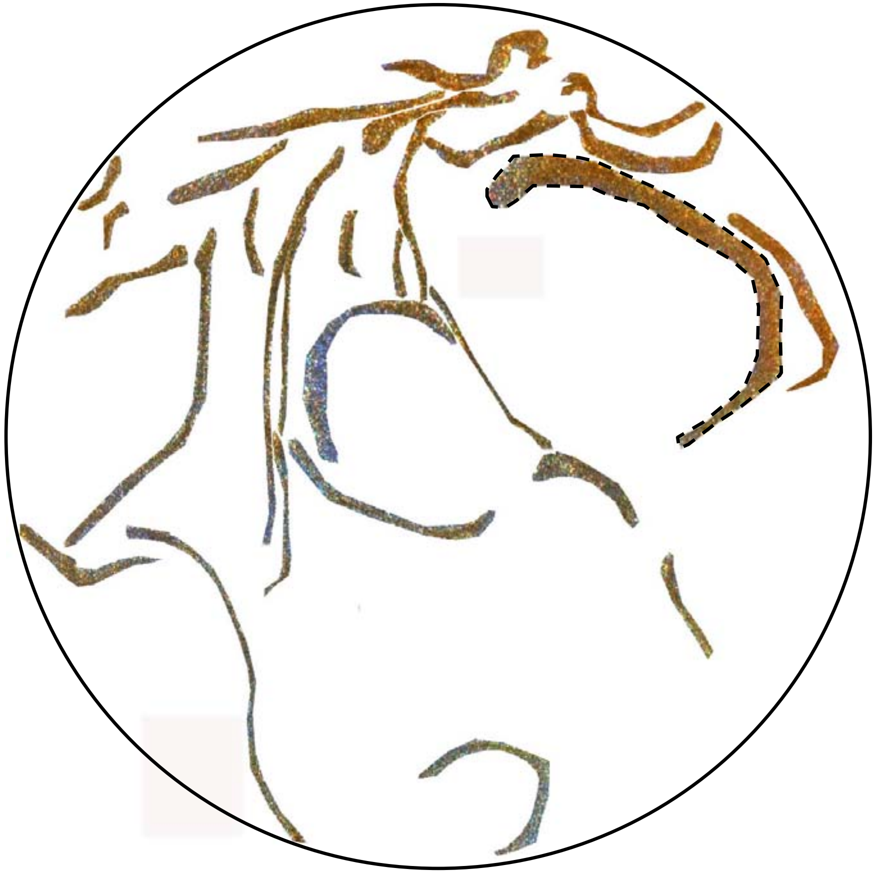

Extraction of sheet-like plumes

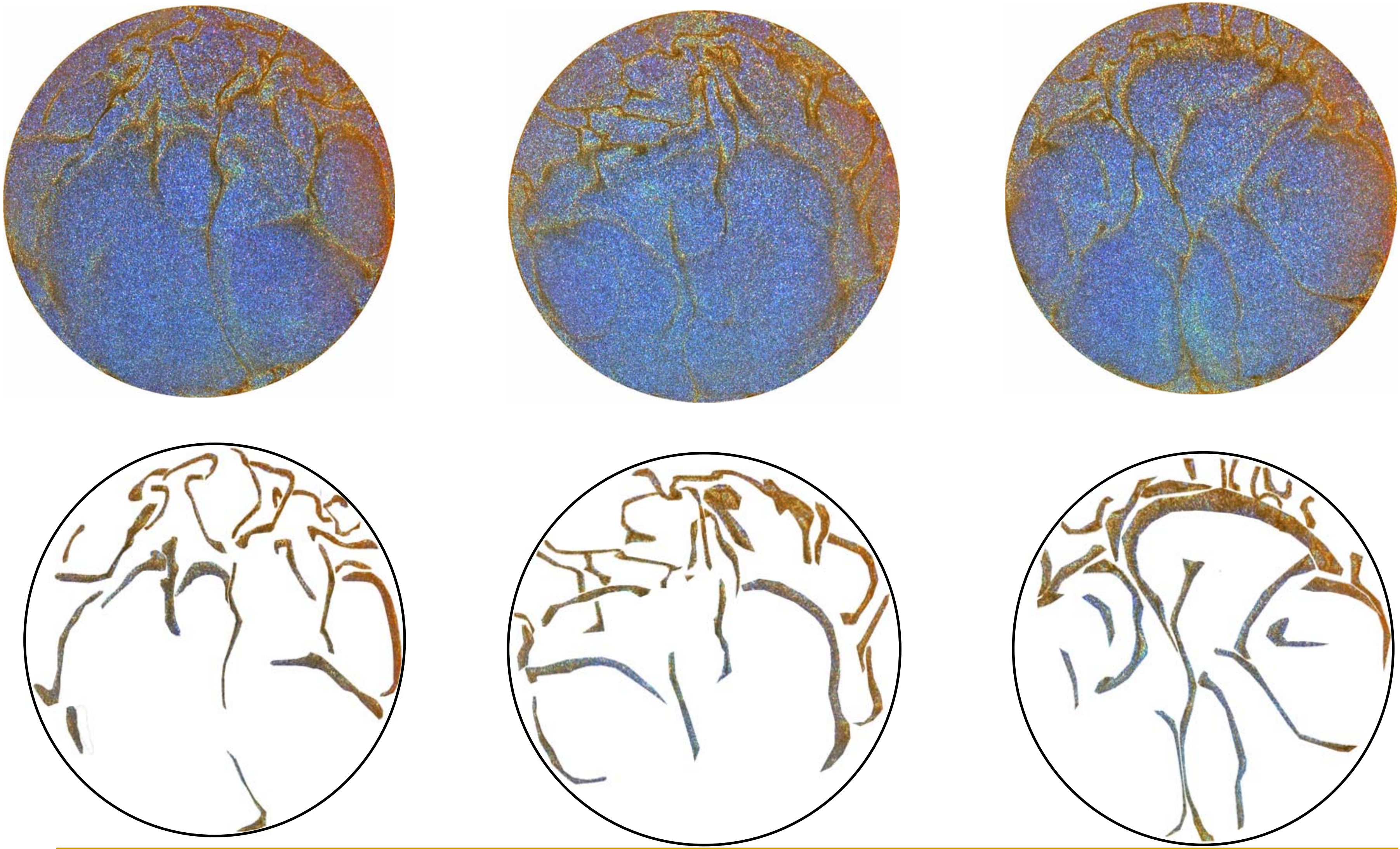

Geometric characteristics: Area

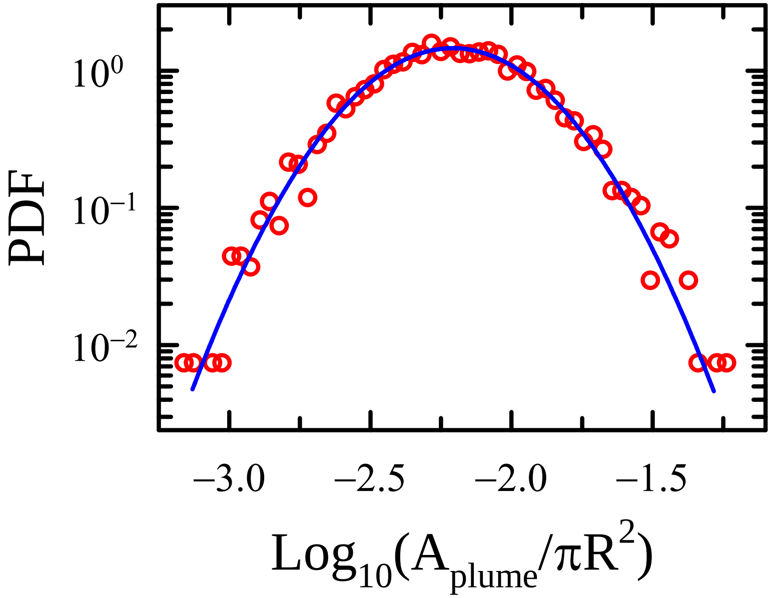

4001 plumes extracted from 200 images.

Areas of plumes follow log-normal distribution: both sheet-like and mush-like plumes (Zhou and Xia, PRL 2002).

Geometric characteristics: Length

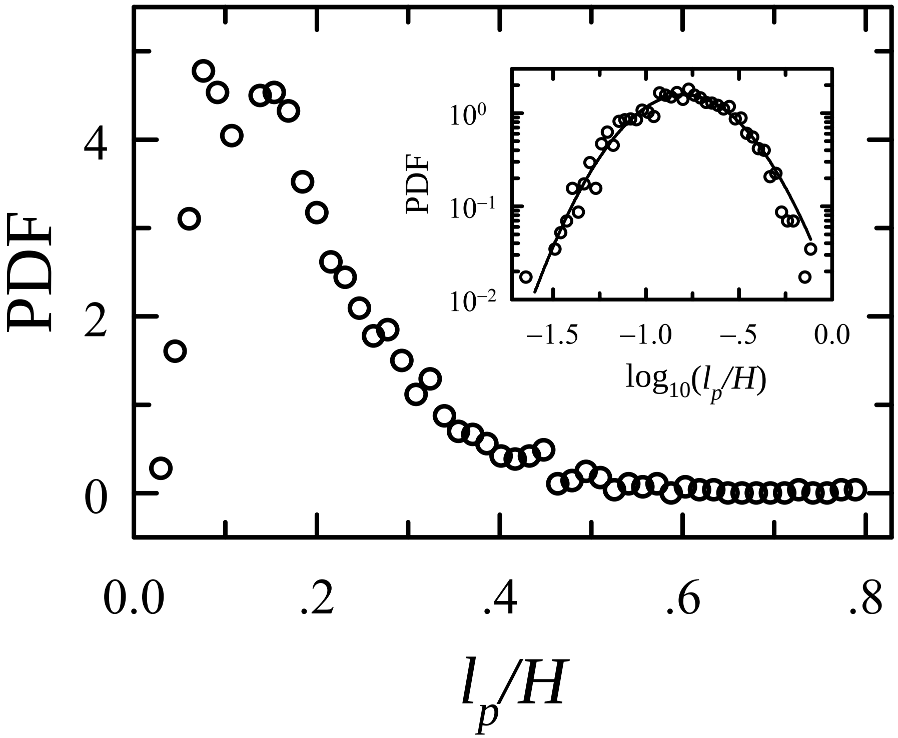

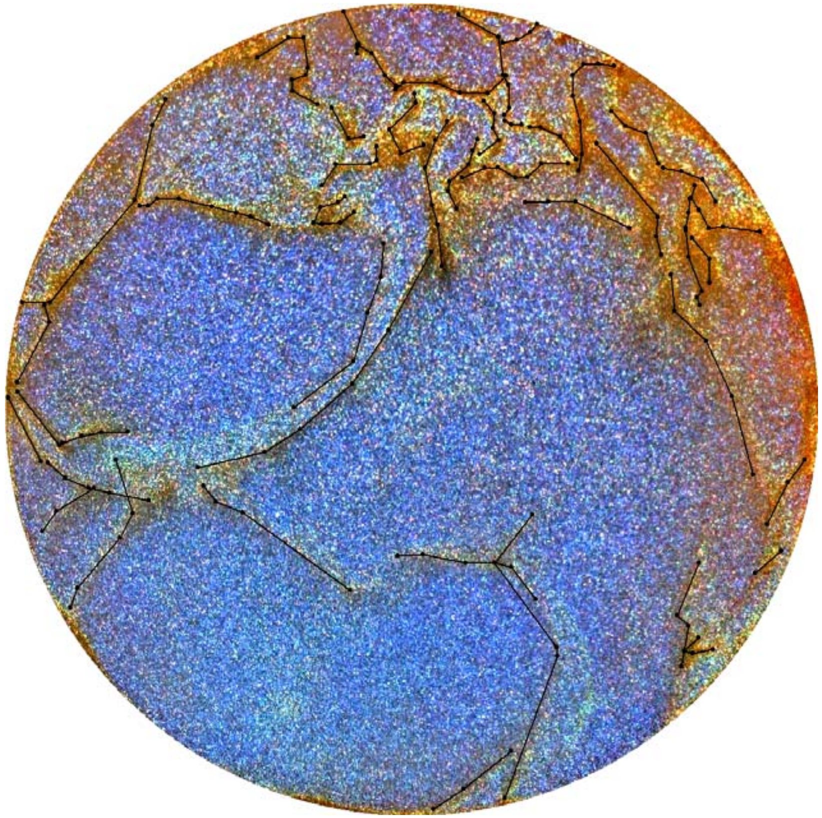

The lengths of sheet-like plumes also follow log-normal distribution.

Temperature of a plume

Red-Green-Blue (RGB)

↓

Hue-Saturation-Intensity (HSI)

Hue: a measure of the peak wavelength → **temperature**

Saturation: a measure of the color contrast

Intensity: a measure of the total light intensity

Plumes statistics

‘heat’ contained in a plume

$$Q_p = \sum c_p(T_i)\rho(T_i)S_{pix}(T_i - T_0)$$

Area of a pixel:

$$S_{pix} = 0.16 \times 0.16 mm^2$$

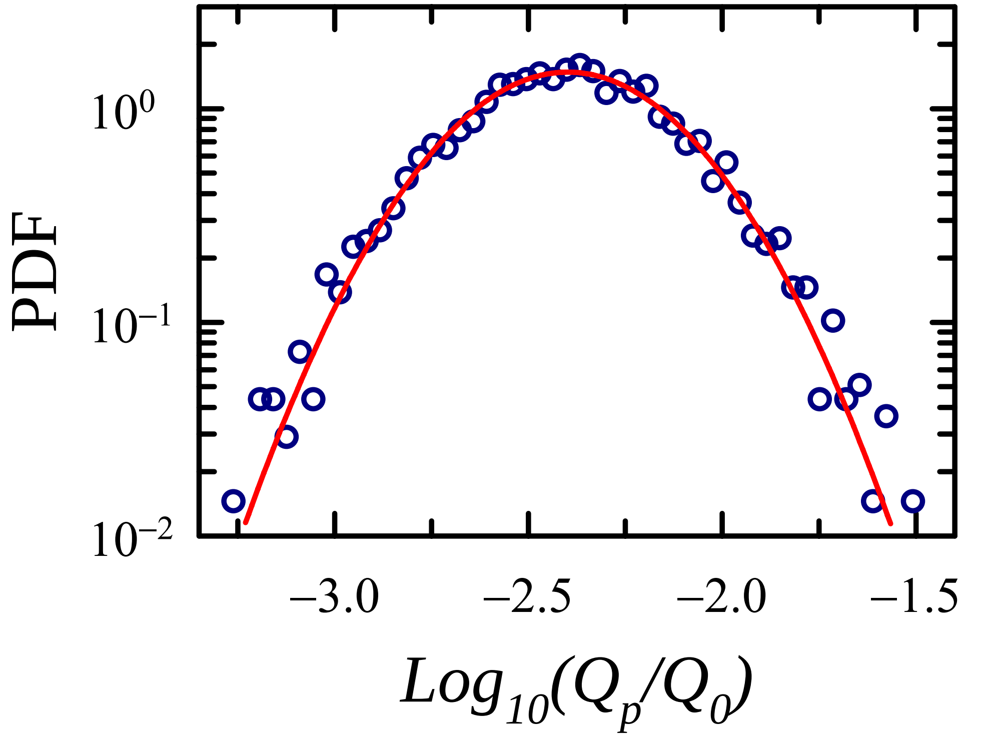

‘heat’ contained in a plume also has log-normal distribution.

The distribution of Q_p is determined by the geometric properties of the plume

Mush-like plumes

2.5 cm from top plate

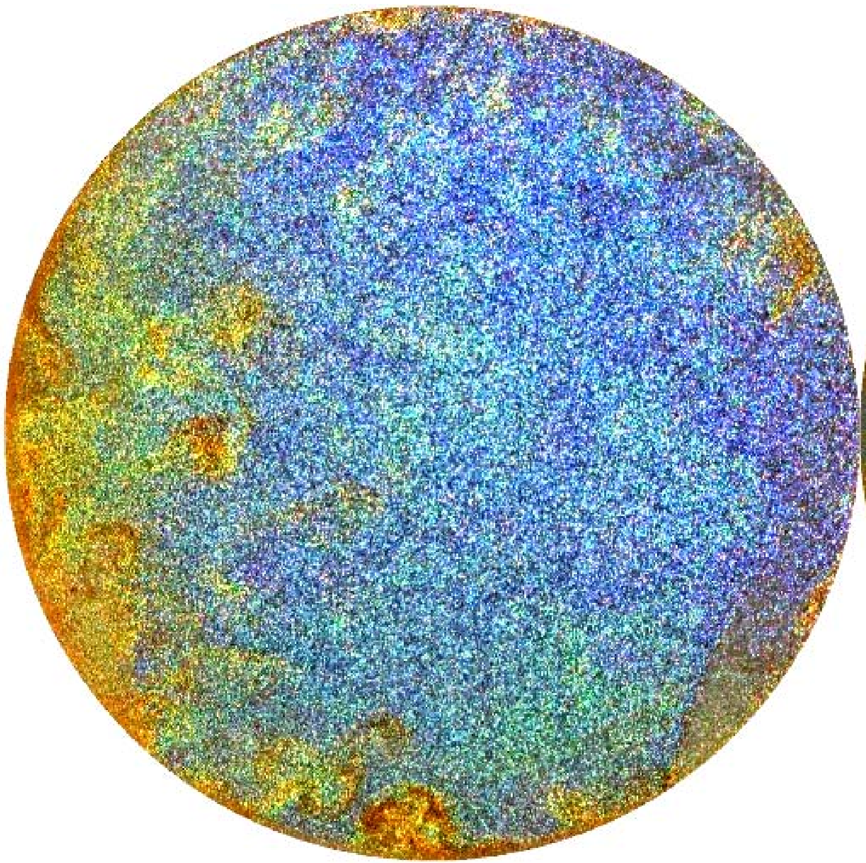

9.3 cm from top plate

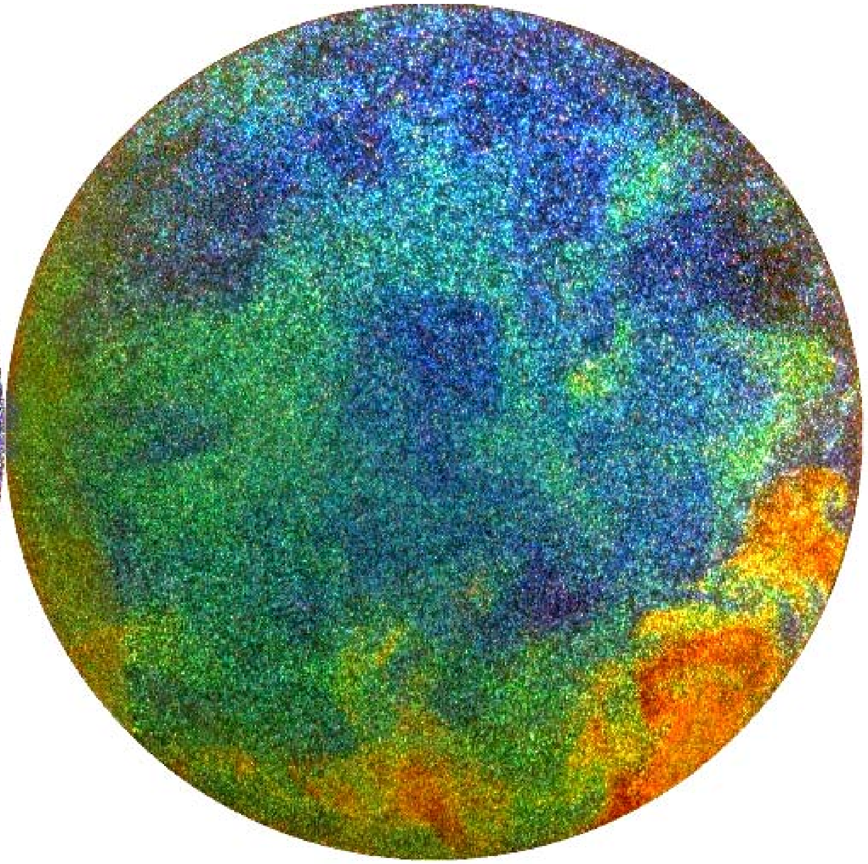

Mush like plumes were observed in bulk region.

Vortical plumes

Long-exposure shot gives both temperature and trajectories of the TLC particles.

2.5 cm from top plate

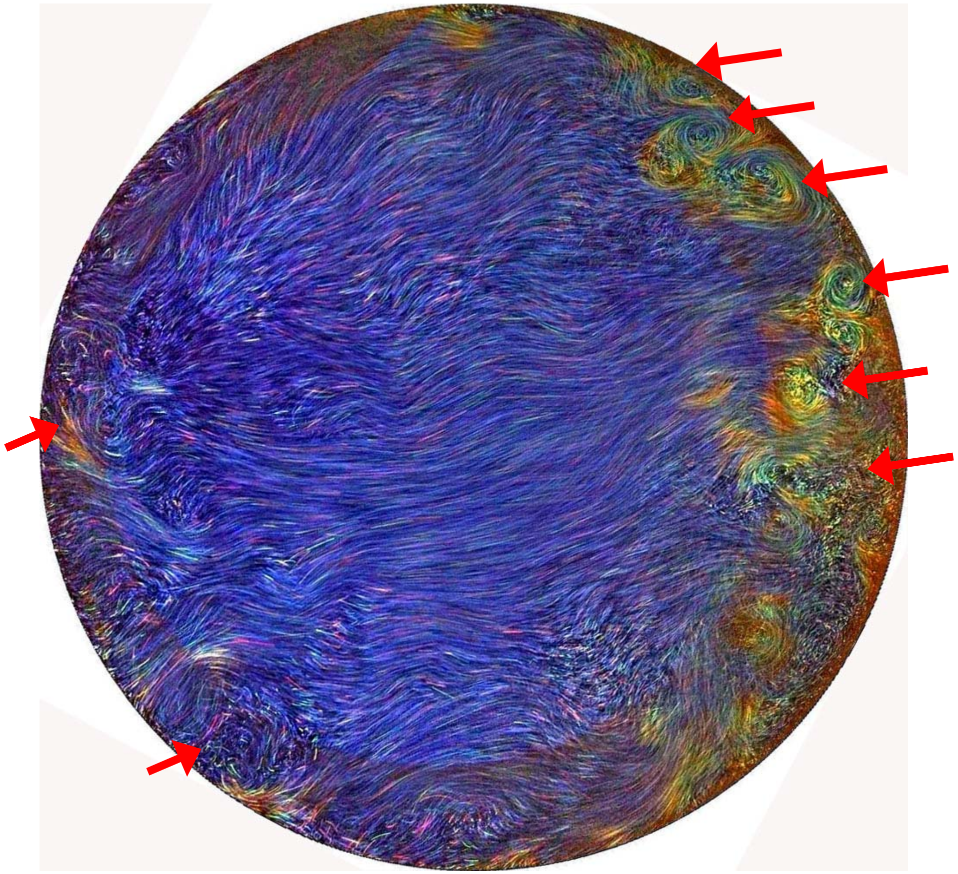

9.3 cm from top plate

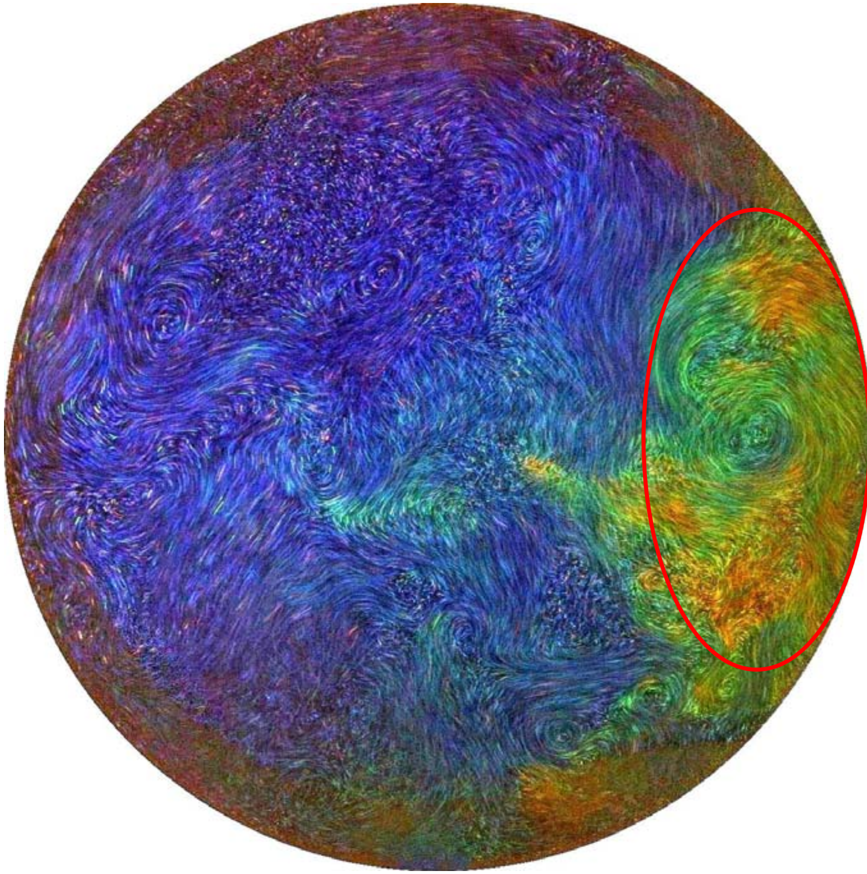

Mush like plumes have intense vortical structures!

Where does vorticity come from?

Formation of mushroom-like plumes: interaction between sheet like plumes

3 mm from top plate

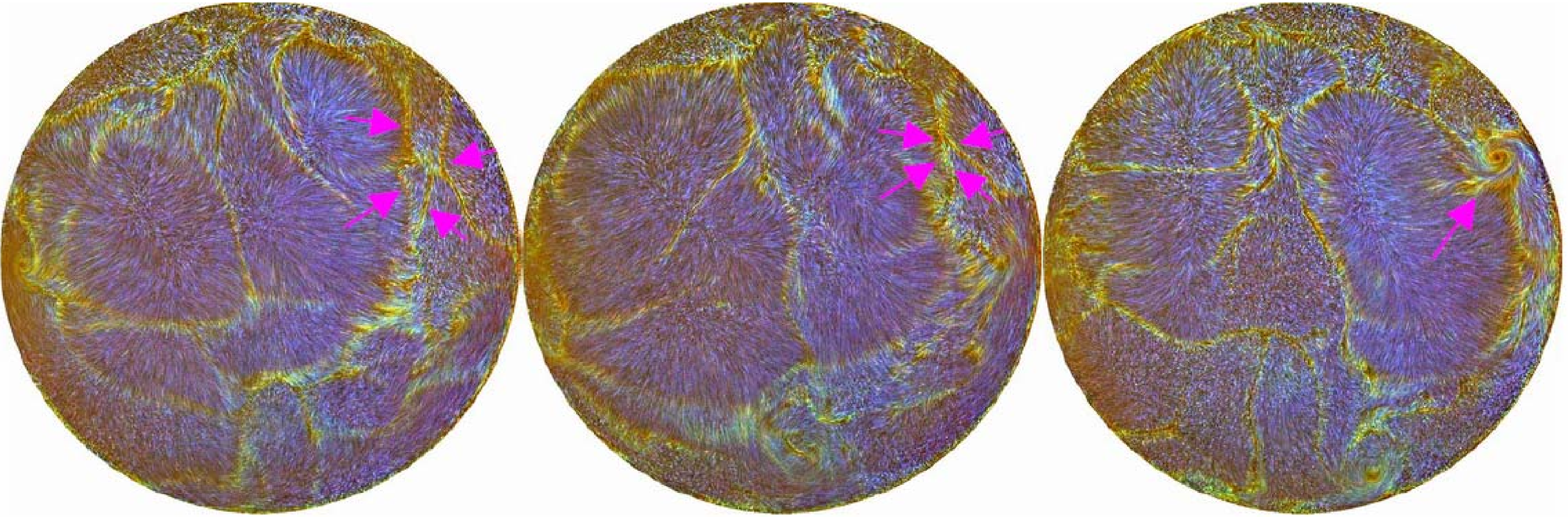

Sheet-like plumes collide and convolute to form swirls that spiral down to become mushroom-lime plumes.

Plume clustering

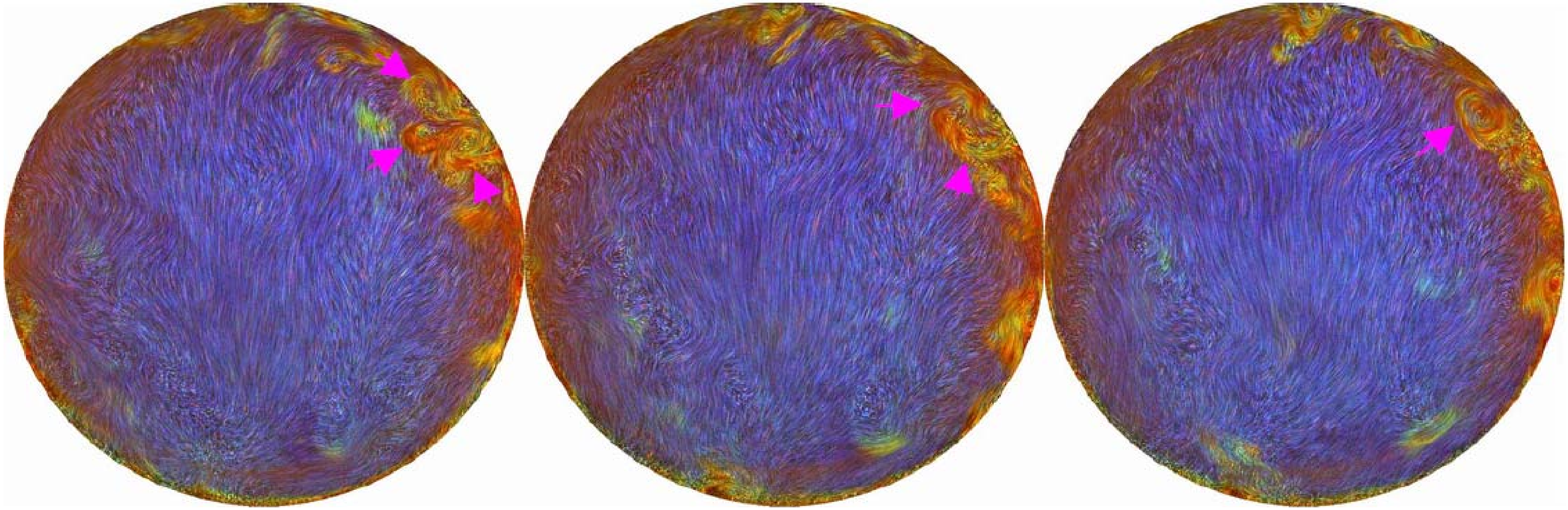

Plumes merge and cluster as they move upward/downward.

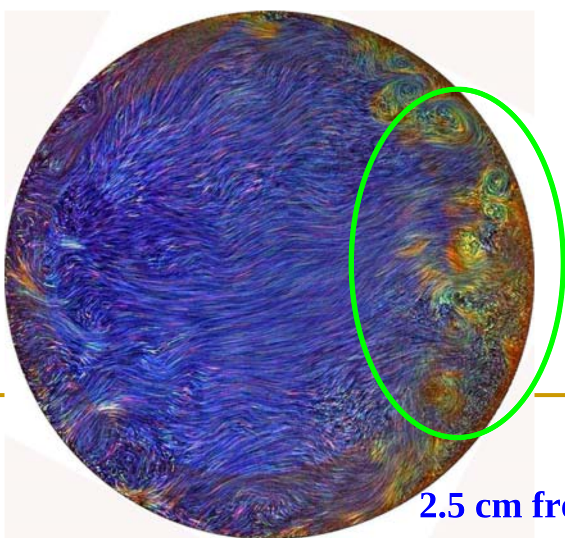

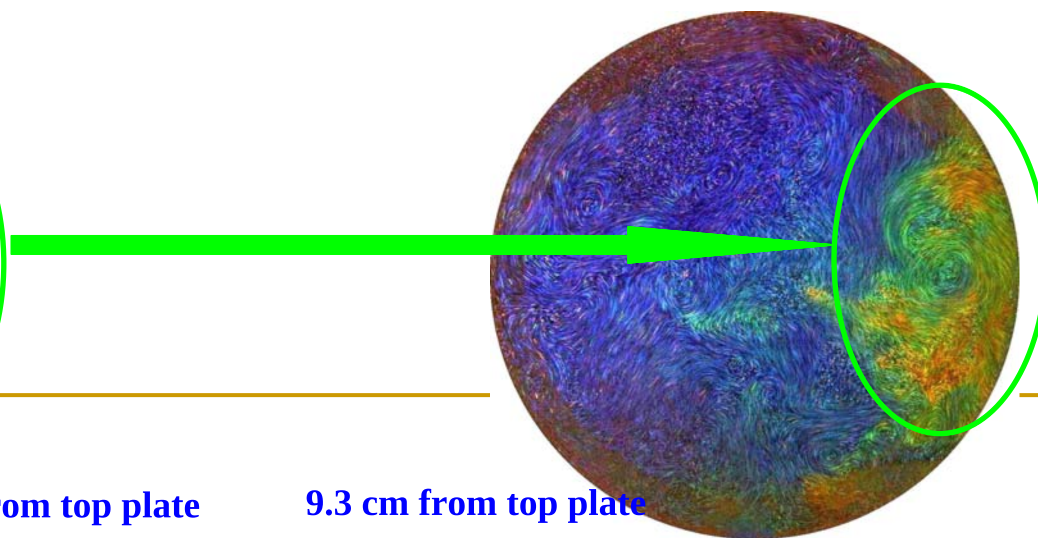

2.5 cm from top plate

9.3 cm from top plate

Morphological evolution of sheet-like to mushroom-like plumes

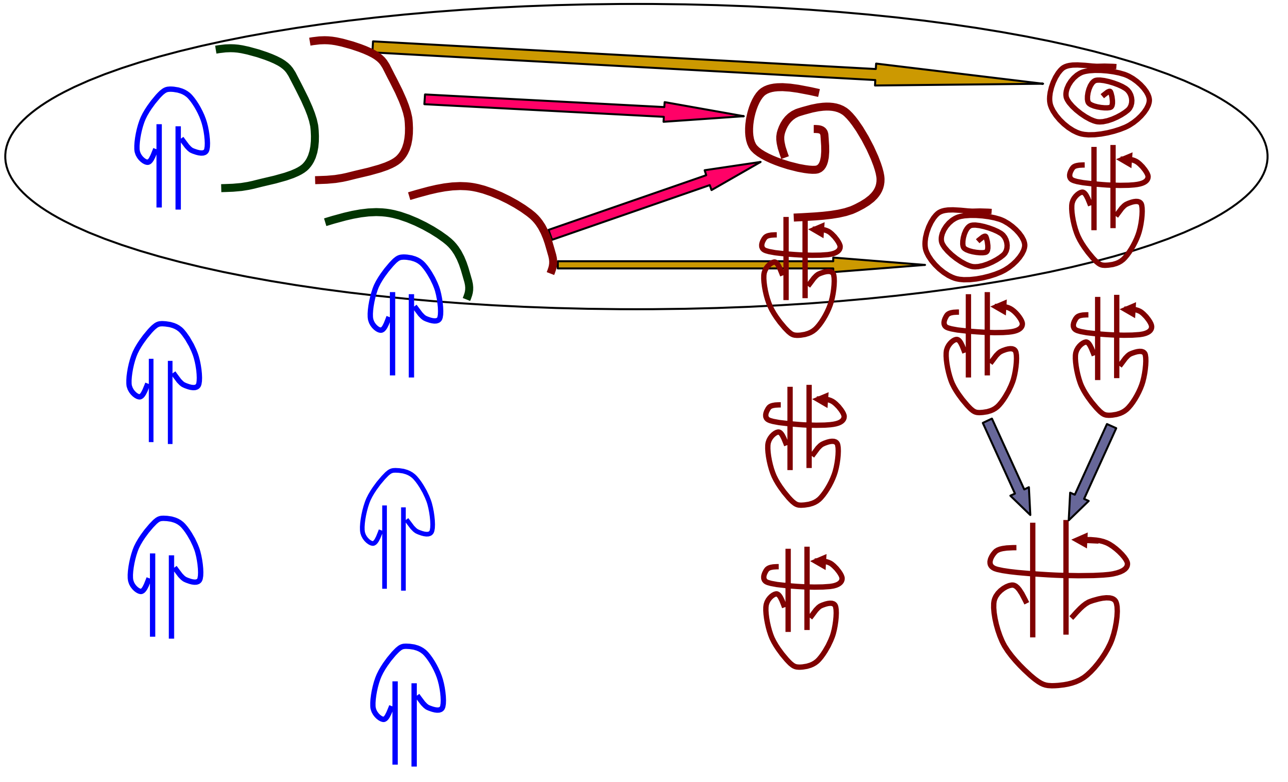

Simultaneous vorticity & temperature measurement

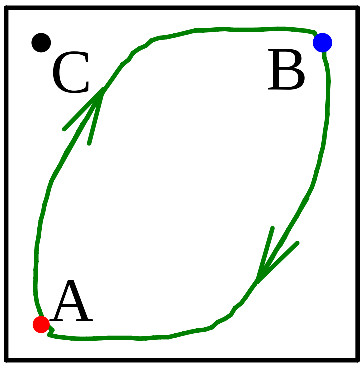

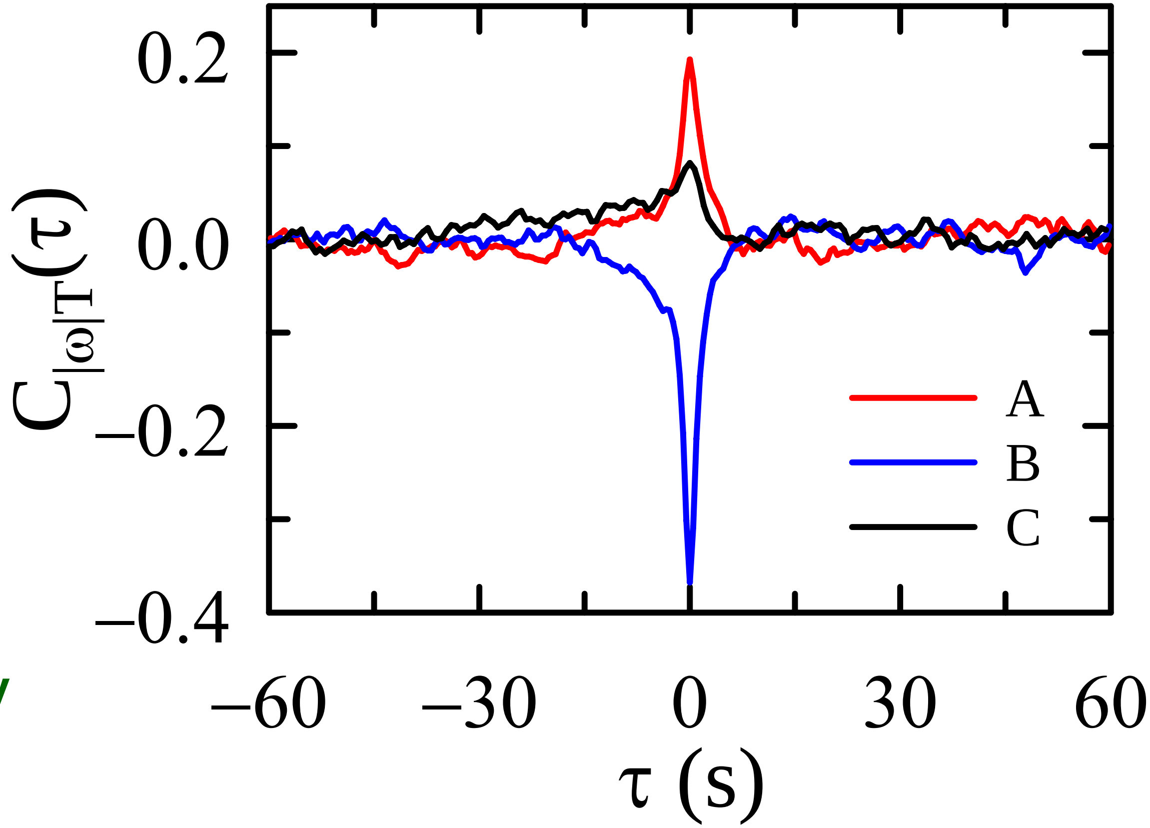

The fluctuations of vertical vorticity and temperature are strongly correlated.

PDF of temperature, velocity and vorticity

Temperature: Exponential

Velocity: Gaussian

Vorticity share the same characteristics with temperature rather than with velocity.

Ra-dependence of vorticity and temperature fluctuations share similar behavior.

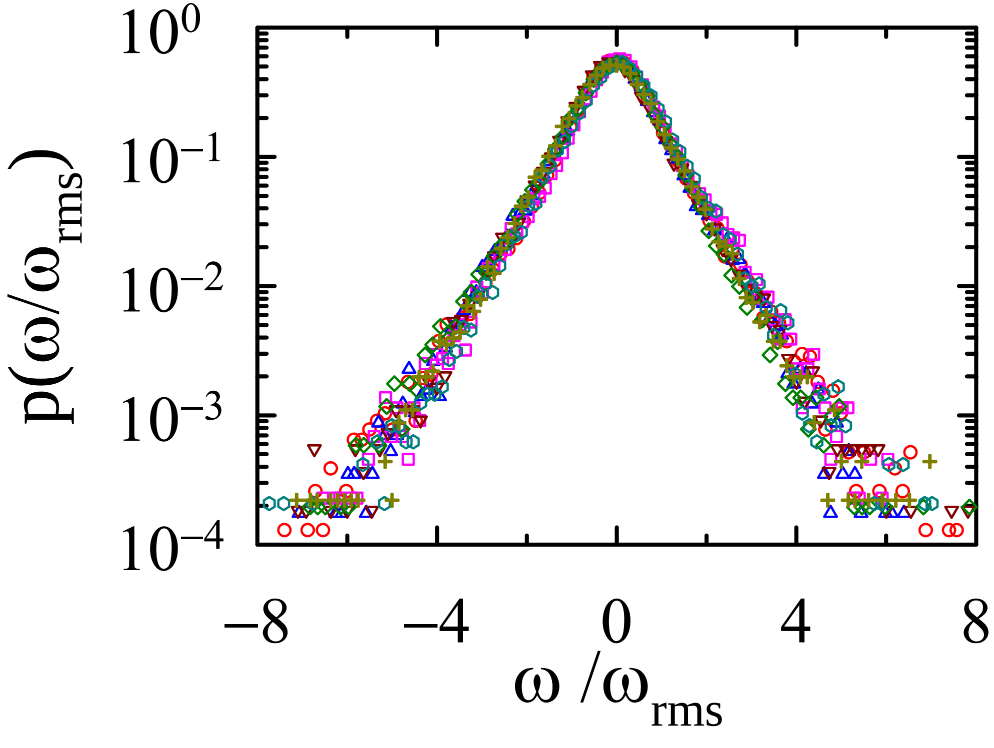

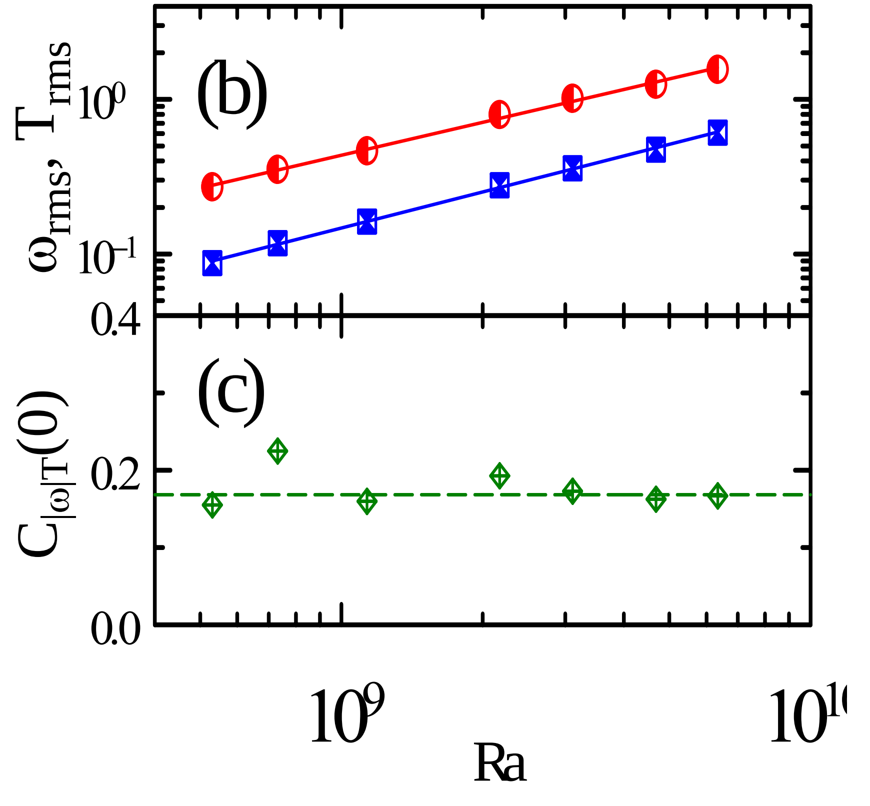

Vorticity profile

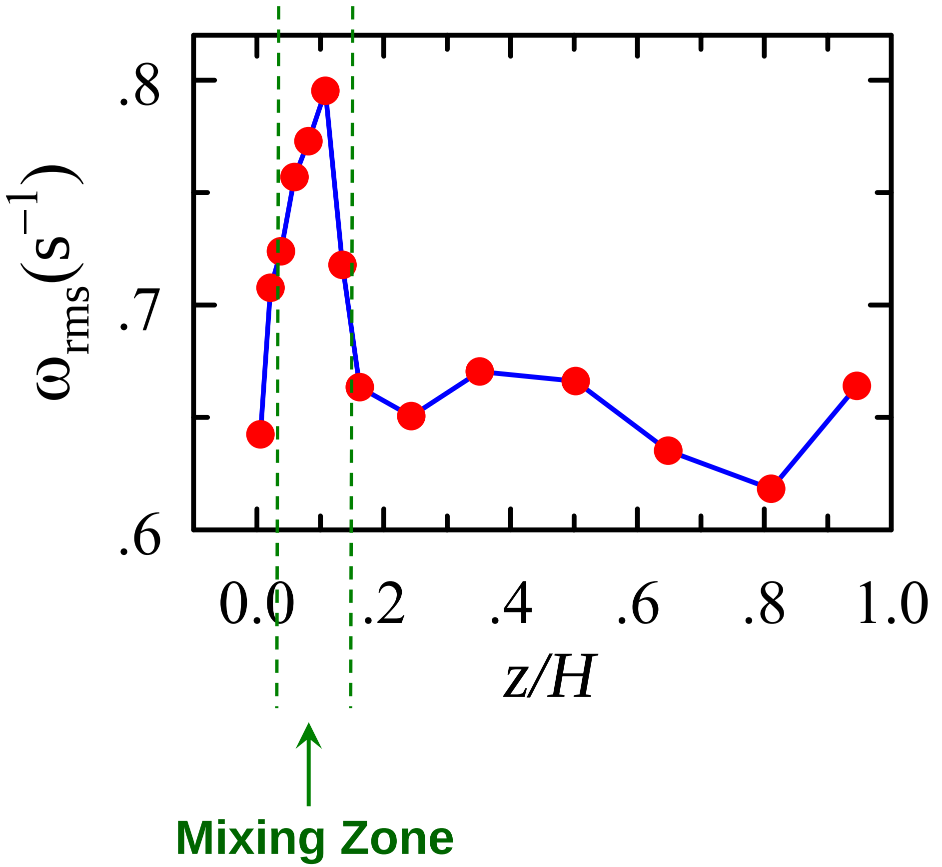

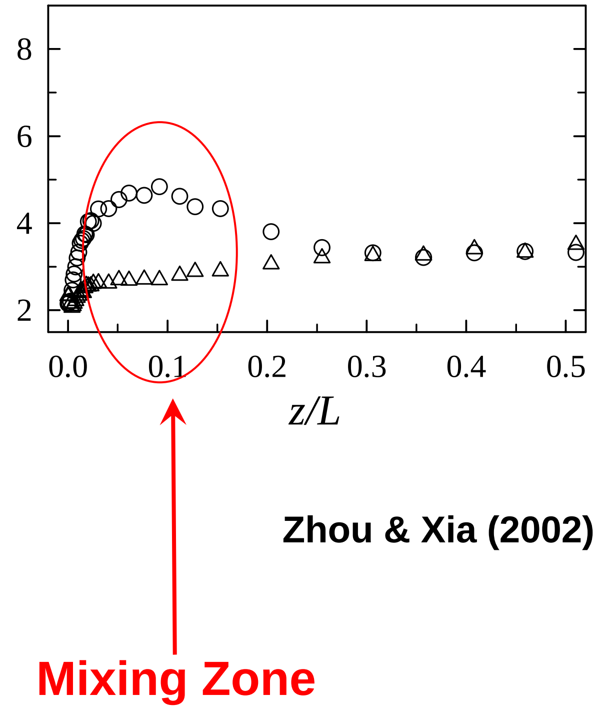

Zhou & Xia (2002)

The maximum ω_{rms} suggests that strong vorticity fluctuations are associated with merging and clustering of plumes.

The mixing zone is roughly the same as that found from the skewness of plus and minus temperature increments.

Summary for Part 3

- Individual sheetlike plumes are extracted as 2D individual geometrical and thermal objects and their area, circumference, and `heat content' are found to all exhibit log-normal distributions.

- As the sheetlike plumes move across the plate they collide and convolute into spiraling swirls. These swirls then spiral downward to become mushroom-like plumes accompanied by strong vertical vorticity.

- The measured vorticity profile reveals a mixing region within which most of plume merging and clustering take place.

- The fluctuating vorticity is found to have the same exponential distribution and scaling behavior as the fluctuating temperature.